University of Tennessee, Knoxville

TRACE: Tennessee Research and Creative Exchange

Masters Theses

Graduate School

8-2006

Characterization of Hypertriglyceridemia in Obese Diabetic TallyHo/Jng Mice

Jennifer Melanie Fortuna
University of Tennessee - Knoxville

Follow this and additional works at: https://trace.tennessee.edu/utk_gradthes

 Part of the Nutrition Commons

Recommended Citation

Fortuna, Jennifer Melanie, "Characterization of Hypertriglyceridemia in Obese Diabetic TallyHo/Jng Mice. " Master's Thesis, University of Tennessee, 2006.
https://trace.tennessee.edu/utk_gradthes/1552

This Thesis is brought to you for free and open access by the Graduate School at TRACE: Tennessee Research and Creative Exchange. It has been accepted for inclusion in Masters Theses by an authorized administrator of TRACE: Tennessee Research and Creative Exchange. For more information, please contact trace@utk.edu.

To the Graduate Council:

I am submitting herewith a thesis written by Jennifer Melanie Fortuna entitled "Characterization of Hypertriglyceridemia in Obese Diabetic TallyHo/Jng Mice." I have examined the final electronic copy of this thesis for form and content and recommend that it be accepted in partial fulfillment of the requirements for the degree of Master of Science, with a major in Nutrition.

Jung Han Kim, Major Professor

We have read this thesis and recommend its acceptance:

James W. Bailey, Lisa Jahns

Accepted for the Council:
Carolyn R. Hodges

Vice Provost and Dean of the Graduate School

(Original signatures are on file with official student records.)

To the Graduate Council:

I am submitting herewith a thesis written by Jennifer Melanie Fortuna entitled “Characterization of Hypertriglyceridemia in Obese Diabetic TallyHo/Jng Mice.” I have examined the final electronic copy of this thesis for form and content and recommend that it be accepted in partial fulfillment of the requirements for the degree of Master of Science with a major in Nutrition.

We have read this thesis
and recommend its acceptance:

Jung Han Kim

James W. Bailey

Lisa Jahns

Accepted for the Council:

Anne Mayhew

Vice Chancellor and Dean of
Graduate Studies

(Original signatures are on file with official student records).

CHARACTERIZATION OF HYPERTRIGLYCERIDEMIA IN OBESE DIABETIC TALLYHO/JNG MICE

A Thesis
Presented for the
Master of Science Degree
The University of Tennessee, Knoxville

Jennifer Melanie Fortuna
August 2006

DEDICATION

This thesis is dedicated to my parents, John and Melanie Fortuna, whose love and support have helped me reach this goal in my life. I thank them for believing in me and for always being there for me. I would also like to thank my brother John and his wife Milissa, my sister Debbie and her husband Blake, and my sister Lisa and her husband Matt. All of you made this possible. A special thanks to my friends as well. I am so blessed and lucky to have you all in my life. Thanks for making me laugh. I would not have made it without you guys.

"I have learned, in whatsoever state I am, therewith to be content. I can do all things through Christ which strengthens me."

Philippians 4:11-13

ACKNOWLEDGEMENTS

I would like to thank everyone who has supported and educated me during both my undergraduate and graduate years at the University of Tennessee-Knoxville. I would especially like to thank **Dr. Jung Han Kim**, my advisor and friend. She gave me my start in research, and I cannot thank her enough for the opportunity. I thank her also for her time and patience with me. She has helped me to not only grow as a researcher but as a person as well. Without her support and mentoring, writing this thesis would have been practically impossible.

I would also like to thank **Dr. James Bailey** (Go Steelers!) and **Lisa Jahns** for serving on my committee. Thank you for offering helpful feedback on this study and for your encouragement and support. I would also like to thank **Dr. Jay Whelan**, my advisor from undergraduate, for his advice and much enthusiasm.

I am also very thankful for having such wonderful people to work with in the lab. Taryn Stewart, Ola Mostafa, Hyoung Kim, and Luan Wang each helped me in some way, either by teaching me laboratory techniques and methods or just being there when I needed someone to talk to. All of you contributed to my success, and I thank you so very much.

Finally, I would like to thank my family and friends. Thank you all for your love and support and for giving me advice when needed. God has blessed me with such wonderful people in my life.

ABSTRACT

Over the past 20 years, a major shift in the type 2 diabetes mellitus (T2DM) epidemic has occurred. Even though the etiology of T2DM has not yet been discovered, insulin resistance, associated with plasma lipid and lipoprotein abnormalities, has shed light to this chronic disease. According to the Centers for Disease Control and Prevention (CDC), 97% of individuals with diabetes have one or more plasma lipid abnormalities, including decreased high density lipoprotein (HDL) cholesterol, a predominance of small dense low density lipoprotein (LDL) particles and hypertriglyceridemia (HTG). Diabetic patients often develop hyperlipidemia at the early stage of the disease and often before the onset of overt hyperglycemia (diabetes). It is also well established that the prevalence of T2DM in the United States is associated with increased prevalence of obesity. The therapeutic plan for T2DM begins with modifications of lifestyle, such as physical activity, changes in diet, weight loss, and smoking cessation (2005 American Diabetes Association clinical guidelines). This is often concomitant with pharmacological therapy. Statins, fibrates, niacin, and thiazolidinediones are commonly used to treat dyslipidemia associated with insulin resistance and T2DM.

The TALLYHO/Jng (TH) mouse strain is a newly established polygenic inbred model for T2DM that shows obesity, hyperinsulinemia, insulin resistance, hyperglycemia (males), and dyslipidemia with the early onset of HTG. Previous work in this laboratory has revealed that insulin resistance is profoundly associated with HTG in TH male mice. The aim of the present study was to characterize the pathogenesis of HTG in TH mice and test the hypothesis that lowering the plasma lipid levels will improve insulin resistance and glucose metabolism in this model.

In vivo studies indicated that the very low density lipoprotein-triglyceride (VLDL-TG) production from liver was not significantly altered in TH mice compared to control B6 mice. On the other hand, TH mice showed a significantly increased residual percentage of injected [^{3}H] TG-labeled VLDL at all sampling times compared to B6 mice, indicating slower VLDL-TG clearance rate in TH mice. In support of the slowed VLDL-TG clearance rate in TH mice, we found

evidence of hepatic over-expression of the Apo C-III gene in TH mice compared to the age- and sex-matched B6 mice. Finally, addition of a drug bezafibrate, known to selectively lower plasma lipid levels without changing plasma glucose levels, to the diet significantly reduced plasma TG concentrations in both B6 and TH mice. Despite the remarkable decrease in plasma TG levels, either glucose tolerance or uptake was not improved in TH mice.

In summary, the HTG appears to be due to a defect in triglyceride-rich lipoprotein clearance in TH mice, and overproduction of Apo C-III may be in part involved in the pathogenesis. Further, the HTG is not likely the primary defect for the impaired insulin action in TH mice. These results shed light on the mechanism underlying the HTG in obese type 2 diabetic TH mice, which may contribute to understanding the pathophysiology of diabetic HTG in humans and ultimately provide biochemical targets for the intervention.

TABLE OF CONTENTS

LIST OF FIGURES

Figure Page

CHAPTER 1: INTRODUCTION

It is well established that the prevalence of diabetes has increased worldwide (1). Between 1980 and 2004, the number of individuals with diabetes increased from 5.8 million to 14.6 million, and almost 40% of people aged 65 years or older have diabetes (2). While 20.8 million Americans have diabetes, 6.2 million cases go undiagnosed. According to Gerberding of the CDC, "new evidence shows that 1 in 3 Americans born in 2000 will develop diabetes sometime during their lifetime" (3). Type 2 diabetes mellitus (T2DM) is the most common form of human diabetes, accounting for approximately 90% of cases (4). Researchers believe that the rising prevalence of diabetes worldwide is associated with increases in the prevalence of obesity and sedentary lifestyle (5).

Diabetes mellitus (DM) can be defined as a group of diseases characterized by high levels of blood glucose resulting from defects in insulin production, insulin action, or both (6). Further, 97% of adults with diabetes have one or more lipid alterations characterized by increased fasting triglyceride (TG), small dense low-density lipoprotein (LDL), and low high-density lipoprotein (HDL) cholesterol (1, 7). Diabetic patients often develop hypertriglyceridemia (HTG) at the early stage of the disease, before the onset of overt hyperglycemia. Recent evidence has demonstrated that HTG is an independent risk factor for coronary heart disease, the prominent cause of diabetic deaths (8).

Genetic animal models have been valuable resources for T2DM research, and few polygenic rodent models, where multiple genes are involved in the development of the disease, have been developed (9). These models include the Goto-Kakizaki (GK), Otsuka Long-Evans Tokushima Fatty (OLETF) rats, Spontaneously Diabetic Torii (SDT) rats, the Nagoya-Shibata-Yasuda (NSY) mice, the Tsumura-Suzuki-Obese-Diabetes (TSOD) mice (10) and the NZO/NON F1 hybrid mice (11).

The TALLYHO/Jng (TH) mouse strain is a newly established polygenic inbred model for T2DM, derived from two deviant male mice showing polyuria and glucosuria in an outbred colony (12). TH mice are characterized by various physiological features, including obesity,

hyperinsulinemia, insulin resistance, hyperglycemia (males), and dyslipidemia associated with increased TG, free fatty acids, and cholesterol levels (12). Our longitudinal study has revealed that insulin resistance is profoundly associated with HTG in TH male mice, and the HTG preceded overt diabetes in this model.

The aim of the present study was to characterize the pathogenesis of HTG in TH mice and test the hypothesis that lowering the plasma lipid levels will improve insulin resistance and glucose metabolism in this model. This study will shed light on the mechanism underlying the HTG in obese type 2 diabetic TH mice and contribute to understanding the pathophysiology of diabetic HTG in humans. This will ultimately provide biochemical targets for the intervention.

CHAPTER 2: LITERATURE REVIEW

I. DIABETES: THE NEW EPIDEMIC

According to the Center for Disease Control and Prevention (CDC), diabetes is the 6th leading cause of associated death in the United States (US). In 2002 alone, the number of deaths resulting from diabetes included 73,249 (13). Approximately 800,000 new cases of diabetes are detected every year, or 2,200 per day (14, 15). While 20.8 million Americans have diabetes, 6.2 million cases go undiagnosed. According to Gerberding of the CDC, "new evidence shows that 1 in 3 Americans born in 2000 will develop diabetes sometime during their lifetime" (3). Researchers believe that the rising prevalence of diabetes is associated with increases in the prevalence of obesity and sedentary lifestyle (5). The National Health and Nutrition Examination Survey (NHANES), using measured heights and weights, shows that from 1999-2002 an estimated 65% of U.S. adults are either overweight or obese. This suggests that the prevalence is 16% higher than the results of the age-adjusted overweight estimates in the NHANES III survey that was completed from 1988-1994 (16). According to the American Dietetic Association (ADA), about 80% of people with type 2 diabetes mellitus (T2DM) are overweight or obese (17). Diabetes mellitus can be defined as a group of diseases characterized by high levels of blood glucose resulting from defects in insulin production, insulin action, or both (6). Overweight and obesity have an adverse relationship with insulin secretion and sensitivity (18).

T2DM accounts for over 90% of the cases of diabetes (4). Unlike type 1A diabetes that is caused by an autoimmune defect in the function of pancreatic beta cells, T2DM has normal pancreas functions, but the peripheral tissues do not recognize glucose as being available for uptake (19). Hodge et al claims that by 2020, approximately 250 million people worldwide will be affected with T2DM (20). This disease usually affects middle aged and older adults, individuals who are overweight, and have a family history of T2DM (21). T2DM is associated with an increased risk for mortality and morbidity (22). Life expectancy is shorter in middle aged individuals with T2DM because T2DM is a risk factor for coronary heart disease (CHD) (23).

Between 1980 and 2004, the number of individuals with diabetes increased from 5.8 million to 14.6 million, and almost 40% of people aged 65 years or older have diabetes (2). According to the CDC National Diabetes Fact Sheet, the number of individuals with diabetes aged 20 or older in the US is approximately 20.6 million in 2005. This statistic represents 9.6% of the population. Approximately 10.9 million men have diabetes in this age group while women make up 9.7 million of this age group (2). The prevalence of diagnosed diabetes among people under the age of 20 is also alarming. In 2005 approximately 176,500 people in the United States under 20 years of age were diagnosed with diabetes. This statistic signifies 0.22% of this population (2). In addition, about 1 in every 400 to 600 children and adolescents has type 1 diabetes. T2DM is also a growing problem for this age group, but data for these trends are unavailable (2).

Race and ethnicity also play a role in defining the total prevalence of diabetes among people aged 20 years or older. In 2005, Non-Hispanic whites made up 13.1 million of this population in the US, and Non-Hispanic blacks included 3.2 million of the population. Approximately 2.5 million Hispanic/Latino Americans have or had diabetes in 2005. Last, there are 99,500 American Indians and Alaska Natives who receive care from the Indian Health Service (IHS). This signifies that 12.8% of American Indians and Alaska Natives aged 20 years or older who receive care from IHS have diabetes (2).

In 2002, the annual health care costs associated with diabetes is approximately $132 billion dollars in the US. This includes both direct and indirect costs. Directs costs include $92 billion, which are due to medical care, insulin, and drugs. Indirect costs are around $40 billion, which are due to disability, work loss, or premature mortality (2).

II. DIABETIC DYSLIPIDEMIA

According to the CDC, 97% of adults with diabetes have one or more lipid abnormalities, such as decreased high density lipoprotein (HDL) cholesterol, a predominance of small dense low density lipoprotein (LDL) particles and increased triglyceride (TG) levels (7, 24). Adult Treatment Panel III (ATP III) and ADA have established the optimal targets of lipid values. The LDL

cholesterol concentration should be less than 2.6 mmol/L (< 100 mg/dL); TG less than 1.7 mmol/L (< 150 mg/dL) and HDL greater than 1.15 mmol/L (> 45 mg/dL) for men, and for women HDL cholesterol should be greater than 1.42 mmol/L (> 55 mg/dL). According to the NHANES III, 85% of patients with T2DM had values of LDL cholesterol greater than 2.6 mmol/L, 42% had TG levels greater than 2.3mmol/L, and 62% of people had levels of HDL cholesterol less than 1.15 mmol/L. Another study conveyed similar results (25).

A survey was conducted on 65,651 people with T2DM from the Basque Country in Spain. These results indicated that 91% of the participants had LDL cholesterol values greater than 2.58 mmol/L, 38.8% had TG values greater than 1.7mmol/L, and 20.8% of the subjects had HDL cholesterol values less than 1.03 mmol/L. These findings clearly suggest that there is a problem with blood lipid concentrations in T2DM patients (25).

It is widely known that a reduced HDL concentration puts individuals at increased risk for coronary heart disease (CHD) (5). HDL particles serve many roles in protecting the heart, such as promotion of cellular cholesterol efflux and direct anti-oxidative and anti-inflammatory properties. Furthermore, low HDL concentrations are frequently associated with increased TG levels, and this association has been positively correlated with an increased risk of CHD. In the Quebec Cardiovascular Study, it was discovered that HDL_2 particles have more cardioprotective effects of high HDL cholesterol levels than HDL_3 particles (7). The subclasses of HDL were determined by first measuring the HDL-cholesterol in the supernatant fraction after precipitation of apoprotein-B containing lipoproteins with heparin/manganese chloride. Then using a 4% solution of low molecular weight dextran sulfate, HDL_2 was precipitated from the HDL fraction. The cholesterol concentration of HDL_3 was then determined and HDL_2 was derived by subtracting HDL_3 from total HDL cholesterol concentrations. Concentrations of HDL cholesterol subfractions may be altered by numerous factors, such as obesity, exercise, and diet (26). However, one limitation in this study is that the association may depend on the specific population being studied. For example, in the Department of Veteran's Affairs HDL Intervention Trial (VA-HIT), it was noted that reduced CHD events in men treated with gemfibrozil were linked with levels of HDL_3.

Therefore, increased levels of HDL_2 and HDL_3 particles may both serve as protective effects against heart disease (7).

People with T2DM and CHD often have small HDL particles. Hyperinsulinemia and hypertriglyceridemia (HTG) are independently associated with low levels of HDL_2 and small HDL particle size (7). Epidemiologic studies suggest a correlation between plasma TG levels and the risk of CHD. A meta-analysis of 17 population-based prospective studies showed that for each 1 mmol/L increase in plasma TG there is a 32% increase in CHD risk for men and a 76% increase in risk for women (27). Effects of triglyceride rich lipoproteins (TRL) such as intermediate density lipoprotein (IDL) and remnant particles may explain for this independent contribution of plasma TG levels to CHD risk. These studies prove that the characteristic dyslipidemia, associated with insulin resistance and T2DM, is positively correlated with an increased risk for cardiovascular disease (CVD) (7).

III. PEROXISOME PROLIFERATOR ACTIVAED RECEPTORS (PPARS)

Classifying the molecular mechanisms of the transducer proteins, which play a role with the metabolic and anabolic pathways, is very important for understanding the energy homeostasis in the human body. This allows added insight in the development of new therapeutic agents for the treatment of chronic metabolic disorders including atherosclerosis and diabetes. Peroxisome proliferator activated receptors (PPARs) are transcriptional factors that are part of the ligand-activated nuclear receptor superfamily. These receptors were identified in the 1990s in rodent models and received their name after peroxisome proliferation. Natural fatty acids and the fibrate class of lowering lipid drugs are known to activate PPARs. PPARs play a major role in controlling the expression of numerous genes that are involved in lipid and glucose metabolism (28).

PPARs' structure is very similar to other nuclear receptors, such as steroid or thyroid receptors. They have an NH_2 terminal region accompanied with a ligand independent transactivation domain. This is usually followed by a DNA binding domain, and at the other end, COOH terminus, a ligand and dimerization domain and a ligand dependent activation domain.

Three major types of PPARs have been discovered thus far, including PPAR-α, PPAR-δ, and PPAR-γ, with each having their own unique characteristics (28).

PPAR-α

PPAR-α is highly expressed in the liver, heart, kidney cortex, and skeletal muscles (22). Activation of PPAR-α has a major effect on lipid oxidation. For example, PPAR-α stimulates the expression of fatty acid transport proteins (FATP) and long chain acyl-CoA synthase in the liver. Furthermore, enzymes that play a role in peroxisomal beta-oxidation, such as acyl-CoA oxidase, are direct targets for PPAR-α. Whereas peroxisomal beta-oxidation does not provide energy, it does shorten very long-chain fatty acids, and this way mitochondrial beta-oxidation can occur. Peroxisomal beta-oxidation also oxidizes molecules, including eicosanoids and xenobiotics (24).

PPAR-α also has other effects. For example, in mitochondrial beta-oxidation, carnitine palmitoly transferase I (CPTI), which is the rate limiting enzyme, is known to be a marker for PPAR-α, although this is much in debate, whether or not CPT1 expression is controlled by PPAR-α. Activation of PPAR-α also induces the expression of medium chain acyl CoA dehydrogenase. This is an important step in mitochondrial beta-oxidation. PPAR-α also stimulates the expression of 3-Hydroxy-3-methyl glutaryl CoA (HMG-CoA) synthase, which is involved in ketone body synthesis.

Activity of pyruvate dehydrogenase kinase 4 (PDK4) is also affected by PPAR-α. PDK4 is a kinase that phosphorylates and inactivates pyruvate dehydrogenase (PDH). If the PDH complex is activated, glucose carbons will be oxidized. On the other hand, if PDH is inactivated in skeletal muscle, the glucose carbons will be used for lactate synthesis. During times of starvation or diabetes, which is associated with a high fatty acid (FA) availability, PPAR-α may be activated, thus having increased PDK4 expression, inactivating PDH and glucose carbon sparing.

The PPAR-α null mice model has helped to establish the physiological role of PPAR-α. Based on this model, numerous enzymes involved in hepatic fatty acid activation, peroxisomal oxidation, and mitochondrial oxidation have been established as markers for PPAR-α (24).

PPAR-α is also known to have a role in cardiac lipid catabolism. For instance, FA oxidative capacity is decreased in heart tissue of these null mice. Myocardial damage and fibrosis may also occur. However, in skeletal muscles, the problem with FA oxidation is less serious because PDK4 acts normally. Research has demonstrated that PPAR-δ is able to make up for this defect (24). PPAR-α null mice model also has a major role in the adaptation to starvation. During starvation, these mice have a fatty liver mainly due to lower fatty acid oxidation capacity. Ketone bodies are also low because the enzyme HMG-CoA synthase is degraded. Glucose metabolism can be severely affected because starvation in these mice leads to definite hypoglycemia. Several reasons show for this. For example, since gluconeogenesis needs a high rate of FA oxidation to supply energy and cofactors, glucose production in the liver may be reduced. Also since ketone bodies are not present, glucose will have to be used (24).

PPAR-α also plays a role in insulin sensitivity. When PPAR-α is activated in obese Zucker rats or lipoatrophic models, insulin sensitivity does improve (24). It is also known that intracellular fatty acids create a problem for insulin-stimulated glucose metabolism (24). If PPAR-α is activated, however, oxidation of FA should increase, thereby lowering the tissue content of lipids and reducing lipotoxicity (24).

The fibrate, such as bezafibrate (BF), is a lipid lowering agent that is a known activator for PPAR-α (29). Both animal and human studies have shown protective effects of fibrates against HTG, hyperglycemia, and insulin resistance. However, changes in a patient's lipid levels will depend on pretreatment lipoprotein status and the effectiveness of the type of fibrate used. In most studies, the obvious effect of fibrates is a decrease in plasma TRL levels. Furthermore, LDL cholesterol levels usually decrease in patients who have increased baseline plasma concentrations. HDL cholesterol levels generally increase when baseline plasma concentrations are low (30).

There are five major mechanisms that explain how the treatment with fibrates can affect lipoprotein status (30).

1. Induction of lipoprotein lipolysis. Increased TRL lipolysis could indicate that there were changes in LPL activity or TRL were more available for lipolysis by LPL due to a reduction of TRL of Apolipoprotein C-III (Apo C-III).
2. Induction of hepatic FA uptake and reduction of hepatic TG production. Studies performed in rodents show that fibrates increase FA uptake and the conversion to acyl-CoA by liver. This is due to the stimulation of FA transporter (FATP) and acyl-CoA synthetase (ACS) activity.
3. Increased removal of LDL particles. Treatment with fibrate helps LDL have a higher affinity for the LDL receptor, which are therefore broken down faster.
4. Decreased plasma TRL. A decrease in plasma TRL levels may lower neutral lipid exchange between VLDL and HDL.
5. Increase in HDL production and the stimulation of reverse cholesterol transport. Fibrate treatment may increase the production of Apo A-I and Apo A-II gene expression in liver, therefore contributing to the increase of HDL levels and a more effective reverse cholesterol transport (30).

BF is an effective nonselective activator for PPAR-α. Taniguchi et al (31) investigated the effects of BF treatment on plasma glucose, insulin, total cholesterol, and TG levels. The subjects included non-obese Japanese type 2 diabetic patients whose age ranged from 42-75. With regard to TG levels, BF treatment reduced serum TG levels significantly. Fasting insulin and fasting glucose both decreased significantly after BF treatment. While HDL cholesterol significantly increased, total cholesterol levels were unchanged throughout the study. BF treatment also improved insulin resistance and fasting insulin levels without affecting insulin secretion in the study subjects.

Jia et al (29) examined the effects of BF on diabetic Otsuka Long-Evans Tokushima Fatty (OLETF) rats and control Long Evans Tokushima Otsuka (LETO) rats. Administration of BF significantly decreased serum TG levels in the OLETF rats. BF treatment, however, exhibited very minor effects on improving insulin sensitivity in OLETF rats.

PPAR-γ

Ligands for PPAR-γ are unsaturated fatty acids such as oleate, linoleate, eicosapentaenoic, and arachidonic acid, and a prostanoid named 15-deoxy-δ-12, 14-prostaglandin J2 (24). Thiazolidinediones (TZD) are also included in this group (24).

Lipid storage and insulin sensitivity are regulated by PPAR-γ. When PPAR-γ is activated, it induces the storage of FAs into mature adipocytes through several ways: LPL stimulation; intracellular FA transport stimulation; FAs activation via acyl-CoA synthase and FA esterification (24).

PPAR-γ also plays a role in regulation of insulin sensitivity. PPAR-γ transgenic mice were resistant to high fat diet induced insulin resistance (24). TZDs are strong compounds that reduce hyperglycemia, hyperinsulinemia, and HTG, characteristics that are often seen in patients with T2DM and in animal models of T2DM. TZDs role is to improve insulin sensitivity of tissues, especially in skeletal muscle. PPAR-γ is high in skeletal muscle, which is the most important tissue in insulin-dependent glucose utilization. It is demonstrated that the involvement of PPAR-γ in insulin sensitivity comes from the fact that TZDs are potent and specific activators of PPAR-γ (24).

When PPAR-γ is activated, it also controls the expression of products produced by the adipocyte. It does this by reducing leptin expression and activating adiponectin expression, a protein involved in insulin sensitivity. PPAR-γ also stimulates the secretion of a particular protein called PPAR-γ angiopoietin-related gene (PGAR). These proteins play a positive role in vascular development (24).

Although PPAR-γ agonists, TZDs are said to have beneficial effects on insulin sensitivity, there are problems and unresolved questions dealing with this issue. For example, diabetic or obese animals treated with TZDs induce adipocyte proliferation and weight gain (24). This might be due to PPAR-γ being a prominent adipogenic transcription factor. However, increasing the number of adipocytes is not adequate to explain the weight gain. There must be disequilibrium

between energy intake and expense. In animal models, most treatment with TZDs shows a noted food intake increase. Only a slight weight gain could be seen in humans, and this weight was observed in subcutaneous adipose tissue. It is unknown why the excessive weight gain was seen in this particular area (24).

Roles of PPARs are better understood because of ligands such as TZDs or fibrates, but their activation in physiological and pathophysiological circumstances is still unclear. This might explain for the problems and inconsistency that was discussed above.

IV. PATHOGENESIS OF DIABETIC DYSLIPIDEMIA

The etiology of atherogenic dyslipidemia of diabetes is generally associated with altered metabolism of TRLs. TRLs include particles derived from the intestine (chylomicrons (CM) and their remnants) containing Apolipoprotein B (Apo B) 100 and the liver VLDL. Apo B 48 and Apo B 100 separate particles derived from exogenous and endogenous pathways that fall within the same density range. On the other hand, the liver produces a range of Apo B 100 comprised of particles that differ in size and density from large VLDL to LDL. Large buoyant VLDL 1 particles and small dense VLDL 2 particles make up the two primary subclasses of VLDL. The first group, large buoyant VLDL 1 particles seem to play a role in determining plasma TG and Apo B 100 in subjects who have normal lipid levels but also in patients who may have high TG levels. Furthermore, high VLDL 1 TG is the deciding factor of plasma TG levels in T2DM as well (25).

Intermediate-density lipoproteins (IDL) make up VLDL and CM and are found to be atherogenic in humans and in a number of animal models (7). CMs are produced in the intestinal lumen after fat is digested. They are the largest of the lipoproteins and are rich in TG. Their function is to transport lipids from the liver to the peripheral tissue. VLDL is a lipoprotein similar to that of a CM, which contains a high concentration of TG. LDL is known to be atherogenic, carrying the majority of the cholesterol in the blood and supplying cholesterol to the cells. On the other hand, high levels of HDL are correlated with decreased risk for CHD. The function of HDL is to facilitate the transfer of cholesterol from atherogenic lipoproteins and peripheral tissues to the liver (32).

An increased production of small dense LDL particles may also be a consequence from increased hepatic production and/or delayed clearance from plasma of large VLDL. There have been seven different LDL subspecies reported. They all differ in their metabolic behavior and physiological roles. There is an association between plasma VLDL levels and increased density and decreased size of LDL. Furthermore, the LDL size and density are negatively associated with plasma levels of HDL particularly the HDL_2 subclass. A number of steps, such as lipolysis, play a role in the intricate process involving small dense LDL particles and larger VLDL precursors of LDL. Also, a larger accumulation of small dense LDL particles may result from the interaction involving cholesteryl ester transfer protein and the hydrolysis of TG and plasma lipoproteins by hepatic lipase (HL) (7).

The make-up of HDL particles is very diverse and includes several subclasses that vary in diameter and density. Classes include small dense $HDL_{3c,}$ $HDL_{3b,}$ and HDL_{3a} and large HDL_{2a} and $HDL_{2b.}$ It is suggested that HDL is reduced in patients with T2DM and who are insulin resistant. Although the mechanism is unclear, it seems to result from the increased transfer of cholesterol from HDL to TRLs, including reciprocal transfer of TG to HDL. The reduced HDL levels in plasma observed in patients with T2DM arise from the reductions in the HDL_{2b} subclass or from the increases seen in the smaller dense HDL_{3c} and HDL_{3b} subclasses. (7).

In T2DM, insulin resistance occurs when muscle, fat, and liver cells do not respond to the action of insulin properly. The pancreas has trouble keeping up with the body's need for insulin, and as a result high levels of insulin are shown in the bloodstream (33). In patients with T2DM and who are also insulin resistant, there is an increased efflux of free fatty acid (FFA) from adipose tissue and impaired insulin mediated skeletal muscle uptake of FFA increase FFA flux to the liver (34). Epidemiologic studies have also shown a relationship between plasma FFA levels and insulin resistance. In individuals who are insulin resistant, FFA in the form of TG are accumulated in non-adipose tissues including the muscle, liver, heart, and pancreas.

Lipoprotein Lipase (LPL)

Lipoprotein lipase (LPL) is one of the most important enzymes involved in the metabolism of TRLs. LPL is normally synthesized in most extrahepatic tissues, mainly in adipose tissue and muscle (35). LPL regulates plasma lipoprotein levels through the hydrolysis of TG in CM and VLDL at the luminal side of the endothelium. FFAs are generated through this process and are used as an energy source in the muscle or stored as fat in adipose tissue. LPL also catalyzes the hydrolysis of HDL phospholipids and TG (36). Moreover, LPL plays a role in the hepatic clearance of TRL by regulating receptor mediated uptake of atherogenic LP particles. Therefore, LPL is said to have anti-atherogenic effects. On the other hand, LPL located on the subendothelially side may have pro-atherogenic effects by increasing oxidative susceptibility of LDL to help with TRL uptake by macrophages. This action may increase the chances of foam cell formation, which is a characteristic of atherogenesis (37).

Diabetes is linked with a deficiency in LPL and the development of HTG. Most studies involving the regulation of LPL have been performed in control rats, streptozotocin-induced diabetic rats, and diabetic rats treated chronically or with a single dose of insulin. Tavangar et al demonstrated that diabetes decreased LPL activity in adipose tissue by decreasing immunoreactive LPL protein and the steady-state levels of LPL mRNA. However the main factor is that diabetes reduces the catalytic activity of LPL (38).

LPL is important during regulation of plasma TG. During the fed state, a high adipose LPL activity along with low activity in the muscle may result in the preferential uptake of hydrolyzed TG by adipose tissue for storage. However, during fasting, high muscle activity and low adipose LPL activity will make plasma TG the leading energy source. Insulin plays an important role in the nutritional regulation of LPL. Under a number of physiological states, there is a strong association between plasma insulin levels and LPL activity in adipose tissue (38). Even so, there are other factors that need to be considered that deal with the relationship between insulin levels and muscle LPL activity because this relationship is not easily understood (38).

Numerous factors play a role in the regulation of LPL. For instance, insulin deficiency, as seen in diabetes, can result in an increase in plasma TG and FFA levels. As a result, FFA levels in the liver will lead to an increase in VLDL synthesis. However, the VLDL synthetic rates improve in prolonged diabetes. Also because of the decrease in LPL activity a potential problem may be detected in the removal of TRL from plasma. When comparing the physical state of the lipoproteins between diabetic animals and normal animals, the TRL from diabetic animals were cleared more slowly. Insulin, however, can help correct the diabetic dyslipidemia that occurs from insulin deficiency. The regulation of LPL in diabetes seems to play a major role in the defect of removing TRL from plasma. In this case, LPL activity in the adipose tissue is low and is not influenced by the absence of insulin. However, the impact that diabetes has on muscle tissue is variable. In cases that study diabetic heart and skeletal muscle, LPL activity can be noted as unchanged, increased, or decreased (38).

The Metabolism of Lipids

Apolipoproteins are proteins that combine with a lipid to form a lipoprotein. They are grouped into four classes: *A*, *B*, *C*, and *E* and a fifth class *D* but is now considered part of A (39). While these proteins have the ability to bind lipids, each class of apolipoproteins has different features. For instance, apolipoproteins can form a relationship with all the different density classes of lipoproteins (LP) and sometimes act as ligands that influence the interaction of LP with cell surface receptors. Furthermore, apolipoproteins play a role in lipid metabolism by serving as cofactors for enzymes. There are nine major apolipoproteins, including Apo A-I, Apo A-II, Apo A-IV, Apo B-48, Apo B-100, Apo C-I, Apo C-II, Apo C-III, and Apo-E (40). These proteins are found in humans, and their genes are isolated on at least three different chromosomes. Gene expression of apolipoproteins is regulated by development, hormones, and diet (41).

LPs are macromolecular complexes containing plasma lipids, especially cholesterol and TG, in the plasma. They also contain hundreds of proteins. These proteins act as a coat for particles that are packed with lipids. TG and cholesteryl esters are present mainly in the particle core whereas the unesterified cholesterol and phospholipids (PL) are located on the surface (42).

There are different kinds of LPs, including CM, VLDL, IDL, LDL and HDL, found in the blood classified accordingly to their density. Also, each LP affects the risk for heart disease in a different way. Abnormalities in plasma lipids and LPs levels contribute to the risk for CAD. However, mutations in the major genes involved in LP metabolism may also contribute to CHD. Genetic studies are providing new insights into disease mechanisms, and these studies, along with biochemical approaches, are giving way to new treatments (43).

Apolipoprotein C-III (Apo C-III)

Apo C-III is mainly synthesized in the liver but also in the intestine (44). Apo C-III is a 8.8 kDa glycoprotein and a 79 amino acid protein (45). Apo C-III is found in human plasma and distributed among TRLs, CM and VLDL, and HDL (46). It has demonstrated that there is a positive correlation between plasma levels of Apo C-III and VLDL-TG concentrations (1). Although the mechanism is unclear, Apo C-III is known to inhibit TRL clearance. Overexpression of Apo C-III links to pronounced HTG in transgenetic mouse through the inhibition of TRL clearance (47). Also, a deficiency in Apo C-III in humans appears to increase the rate of TG clearance from plasma (48). A drug beta,beta'-tetramethylhexadecanedioic acid (MEDICA 16) is capable of reducing TG levels by the suppression of Apo C-III gene expression in rodents (49, 50).

The mechanism by which Apo C-III reduces TG clearance is unclear. It has been proposed that Apo C-III has a negative charge on the surface of LP, and this may inhibit other nonspecific interactions with cell surfaces and maybe other LP. Apo C-III may also interfere with lipolysis because it reduces the affinity of TRL to lipases, such as LPL, or certain surface receptors such as those binding to Apo E or Apo B (45, 49).

On the other hand, Apo E plays a role in the removal of plasma LP. The first phase of TG clearance in peripheral tissues relies on the endothelial bound LPL. LPL prefers to break down TG in CM and VLDL remnants. Almost all CM remnants and VLDL remnants are taken up by the liver and broken down. Apo E may also play a role in the action of LPL and HL. These enzymes play an important role in converting VLDL remnants into LDL (49). Remnants will

accumulate and may result in dysbetalipoproteinemia if there is a lack of Apo E. Dysbetalipoproteinemia is a highly atherogenic mixed hyperlipidemia, which is associated with the accumulation of remnants of TRLs. Apo E plays a role in the binding of these remnants to hepatic lipoprotein receptors (51).

Treatment of Diabetic Dyslipidemia

The therapeutic plan for T2DM begins with modifications of lifestyle, such as physical activity, changes in diet, weight loss, and smoking cessation (7). Epidemiologic and intervention studies have also shown that medical nutrition therapy and physical activity can significantly improve the measurements of diabetic dyslipidemia. Currently, there are recommendations for the management of dyslipidemia in patients with T2DM. For example, evidence shows that a low carbohydrate diet is beneficial in achieving weight loss and improving lipid and LP levels. Even though these behavioral interventions are important for the improvement in diabetic dysipidemia, this is often concomitant with pharmacological therapy. Statins, fibrates, niacin, and TZD are commonly used to treat dyslipidemia associated with insulin resistance and T2DM (7).

Statins (HMG-CoA Reductase Inhibitors)

The primary roles of statins on LP metabolism are controlled by increased LDL receptor activity (7). However reduced hepatic LP secretion also seems to serve an important part. While statins can lower plasma levels of all LDL subclasses and IDL, they can also reduce plasma TG levels and raise HDL cholesterol.

Fibrates (PPAR-α Agonists)

The primary action of fibrates is the reduction of TRL (7). Transcriptional regulation of genes, such as LPL and its activator Apo C-II and inhibitor of Apo C-III, plays an important role in this action. Fibrates also increase HDL via the increased production of HDL apoproteins and reduced transfer of cholesteryl ester from HDL to VLDL. Even though the effects of fibrates on LDL cholesterol are inconsistent, reductions are usually small (7). Fenofibrate treatment has been shown to be effective in normalizing the atherogenic dyslipidemic phenotype in patients with T2DM (7).

The use of statins and fenofibrate taken together have been shown to be highly beneficial in patients with T2DM and combined hyperlipidemia, who exhibit increased LDL cholesterol, low HDL cholesterol, and elevated TG levels. After 24 weeks of both statins and fenofibrate treatment, LDL cholesterol was reduced by 46%, TGs were reduced by 50%, and HDL cholesterol was increased by 22% (5). Small dense LDLs were also reduced by the combined therapy. One limitation concerning this combination therapy is increased toxicity. Recent studies have suggested that the risk seems to be much greater with gemfibrozil than with fenofibrate (7).

Niacin

Niacin has been proven to significantly lower TG levels, increase HDL levels, and increase LDL particle size (7). The mechanism by which niacin helps improve the LP profile is that this water-soluble vitamin reduces fatty acid release from adipose tissue and suppresses hepatic production of VLDL. As a result, TG levels will decrease as well as the number of small dense LDL particles. Studies have shown that niacin also raises HDL levels by reducing uptake via the receptor responsible for intrahepatic degradation of HDL. However, while niacin may provide useful information in the development of new treatments for diabetic lipidemia, it is not recommended because studies have shown that high doses of niacin may worsen glycemic control. A 16-week double blind placebo-controlled study was performed to determine if there was a difference between the placebo and niacin treatment. This study included 148 patients with T2DM and dyslipidemia. The patients were randomly divided to placebo treatment or 1,000 or 1500 mg/day of extended-release niacin. Also, about half the patients received statin therapy along with placebo or niacin treatment. Niacin in amounts of 1000 or 1500 mg/day increased HDL cholesterol by 19 and 24% respectively in relation to the placebo group. The niacin treatment also reduced TG levels by 13 and 28%. Glycemic control in patients changed very little with the 1000 mg dose, except in 4 patients who had to stop participating in the study because of inadequate glycemic control (7).

Thiazolidinediones (TZDs) (PPAR-γ Agonists)

Thiazolidinediones (TZDs) are PPAR-γ agonists that have insulin-sensitizing effects, which can improve glucose control in patients with T2DM. TZDs are not the recommended treatment for dyslipidemia. However, some evidence demonstrates that TZDs may have favorable effects on LP profile and may also be seen as an important improvement for the certain trends of dyslipidemia in diabetic patients. Patients with diabetes often see comparable effects on lipid profiles if given one of PPAR-γ treatments, such as TZDs, rosiglitazone and pioglitzone. TZD treatment often tends to increase total and LDL cholesterol but there is also a constant rise in HDL cholesterol. Pioglitazone therapy often lowers TG levels; TG levels also decrease with rosiglitazone in patients who have elevated baseline TG levels. An observational cohort study was performed to assess TZD therapy. Results indicated that TZD treatment significantly increased LDL particle size and increased the larger HDL_2 subfraction by 24%. Further, rosiglitazone therapy for 8 weeks significantly increased HDL cholesterol levels by 6% and HDL_2 by 12.6% (7). Combination of atorvastatin and rosiglitazone treatment resulted in a 5% increase in HDL was observed. A significant decrease in LDL (-39%) and TG (-27%) was also seen. Pioglitazone has also been known to have a positive impact on atherogenic dyslipidemia in patients with T2DM. In one study comprising of 54 nondiabetic patients with arterial hypertension, small dense LDL levels were elevated in 63% of subjects at baseline. However, after 16 weeks, pioglitazone treatment seemed to reduce dense LDL particles by 22% (7).

TZDs action also decreases the expression of tumor necrosis factor (TNF-α) in adipocytes, cytokines produced from adipose tissue. The functions of TNF-α include impairing insulin receptor signaling, inhibiting LPL, and stimulating lipolysis in fat cells (24). This should lead to an increased availability of FA for muscles and may result in insulin resistance. In animal models of obesity, the gene expression of TNF-α is over-expressed in adipose tissue. Furthermore, interleukin (IL)-6 secreted from adipocytes is negatively correlated to insulin action. The action of TZDs on IL-6 is poorly understood. However, TZDs can decrease IL-6 production by monocytes (24).

V. MODELS FOR DIABETIC DYSLIPIDEMIA

Laboratory animal models exhibit comparable disease states with humans. For this reason, they serve as a powerful aid in human studies. These models overcome difficulties in human studies, such as uncontrolled diets or lifestyle. Animal models share both physiological and genetic similarity with humans. Therefore, the information identified in animal models can be applied to humans (12).

Tsumura, Suzuki, Obese Diabetes (TSOD) Mouse

Tsumura, Suzuki, Obese Diabetes (TSOD) male mice are characterized by polydipisia and polyuria at 2 months old (52). Hyperinsulinemia and hyperglycemia usually follow. After these symptoms, obesity will develop until about 12 months. Severe hypertrophy of pancreatic islets due to proliferation and swelling of beta cells has also been observed in TSOD mice. At 18 months old, the kidney showed thickening of the basement membrane in glomeruli and an increase of the mesangial area. TSOD mice began to experience motor neuropathy at 14 months of age, and most male mice at 17 months of age began to feel weakness in their front and hind paws due to neuron degeneration in the peripheral nerve. The mice at 12 months of age showed a significantly reduced of tail pressure. Using light microscopic and electron microscopic technology, it has been found that the sciatic nerves had a decrease in the density by endoneural fibrosis and loss of these fibers in TSOD mice. Also, there were degenerative changes seen in myelinated fibers, separation of myelin sheaths, and remyelination. Furthermore, the lamellar structure was completely destroyed and microphages were present around myelin sheath (52).

Otsuka Long-Evans Tokushima Fatty (OLETF) Rats

Another spontaneous animal model for T2DM includes the Otsuka Long-Evans Tokushima Fatty (OLETF) rats. OLETF rats show a late onset of chronic and slowly progressive hyperglycemia and polyphagia, which leads to body weight gain, resulting in hyperinsulinemia, HTG, and hyperglycemia (29). Past the age of 40 wks, the rats become hypoinsulinemic, and

they also have defects in insulin secretion. Histologically, the OLETF rats exhibit the progressive fibrosis in the pancreas (29).

Nagoya-Shibata-Yasuda (NSY) Mice

The Nagoya-Shibata-Yasuda (NSY) mice are an inbred model of T2DM, established from the same colony as JcI:ICR. Shibata (19) began selective breeding for glucose tolerance, and shortly thereafter, this NSY strain of mice showed impaired glucose tolerance. The development of diabetes in NSY mice is age dependent, both impaired insulin secretion and action play a role in diabetes and that mild obesity with visceral fat accumulation is linked with this disease (19).

CHAPTER 3: EXPERIMENTAL INVESTIGATIONS

ABSTRACT

The TALLYHO/Jng (TH) mouse strain is a polygenic inbred model for type 2 diabetes mellitus (T2DM) and obesity. TH mice are characterized by insulin resistance, hyperinsulinemia, hyperglycemia (males), obesity, and hypertriglyceridemia (HTG) in combination with increased plasma free fatty acid concentration as well as increased total and high density lipoprotein (HDL) cholesterol levels. Previous work in this laboratory demonstrated that HTG precedes the overt diabetes and is profoundly associated with insulin resistance and hyperglycemia in male TH mice. The aim of the present study is therefore to characterize the pathophysiology of HTG in TH mice and test the hypothesis that lowering the plasma triglyceride (TG) levels will improve insulin resistance and glucose metabolism in this model. HTG could result from either a defect of plasma TG catabolism or hepatic over-production of TG. To examine these questions we determined hepatic TG secretion by the Triton WR-1339 methodology (inhibition of peripheral lipolysis) and exogenous TG clearance (after i.v. injection of radiolabeled very low density lipoprotein-TG (VLDL-TG)). There was no significant increase in TG production in TH mice; however the clearance of VLDL-TG was significantly decreased in these mice compared to C57BL/6J (B6) controls. Moreover, Apolipoprotein C-III (Apo C-III), a key component in the metabolism of plasma TG, gene expression was upregulated in TH mice, while there was no difference in gene expression of lipoprotein lipase, a key enzyme for TG hydrolysis, in TH and B6 mice. A lipid lowering agent, bezafibrate (BF), treatment, significantly reduced plasma TG levels and reduced plasma insulin levels in TH mice. BF, however, did not change glucose tolerance and uptake or glycemia in TH mice. In summary, these results suggest that the HTG in TH mice is caused by reduced VLDL-TG clearance, possibly mediated through increased Apo C-III. Also, the early development of HTG does not appear be directly responsible for diabetes in TH mice.

I. INTRODUCTION

Diabetes and its health related problems are on the rise in the United States. While 20.8 million Americans have diabetes, 6.2 million cases go undiagnosed, and approximately 800,000 new cases of diabetes are detected every year, or 2,200 per day (14, 15). Further, 97% of adults with diabetes have one or more lipid abnormalities, such as decreased high density lipoprotein (HDL) cholesterol, a predominance of small dense low density lipoprotein (LDL) particles and increased triglyceride (TG) levels (7, 24). Type 2 diabetic patients usually have LDL cholesterol levels that are often the same to those in nondiabetic patients (53). Hypertriglyceridemia (HTG), on the other hand, is a major feature of the dyslipidemia found in type 2 diabetes mellitus (T2DM) and typically implies increased levels of very low density lipoprotein (VLDL)-TG (54).

Genetic animal models have been valuable resources for T2DM research, and few polygenic rodent models, where multiple genes are involved in the development of the disease, have been developed (9). These models include the Goto-Kakizaki (GK), Otsuka Long-Evans Tokushima Fatty (OLETF) rats, Spontaneously Diabetic Torii (SDT) rats, the Nagoya-Shibata-Yasuda (NSY) mice, the Tsumura-Suzuki-Obese-Diabetes (TSOD) mice (10) and the NZO/NON F1 hybrid mice (11).

The TALLYHO/Jng (TH) mice are a newly established polygenic model for T2DM characterized by obesity, hyperinsulinemia, insulin resistance, hyperglycemia (males), and dyslipidemia associated with increased TG, free fatty acid, and cholesterol levels (12). Our longitudinal study has revealed that TH male mice exhibit a striking rise in plasma TG levels between 6 and 10 wks of ages where their plasma glucose levels are in the phase of steady rising. On the other hand, normoglycemic TH female mice do not exhibit this TG spike although they maintained HTG compared to B6 control mice (12).

The aim of the present study was to characterize the pathophysiology of HTG in TH mice and test the hypothesis that lowering the plasma TG levels will improve insulin resistance and glucose metabolism in this model.

II. MATERIALS AND METHODS

Animals

Mice were maintained on standard rodent chow with 4% fat [5K54, PMI Feeds, Inc., St. Louis, MO or Harlan Teklad Rodent Diet (W) 8604, WI] ad libitum with free access to water (HCl acidified, pH 2.8-3.2) under controlled temperature and humidity with a 12-hour light and dark cycle. Since the diabetic trait is polygenic in TH mice a simple genetic control of non-diabetic mice does not exist. Therefore, C57BL/6J (B6) inbred mice were used as arbitrary control since B6 is one of the most commonly used strains in diabetes and obesity research and does not develop diabetes when fed standard laboratory chow (12).

All animal studies were carried out with the approval of The University of Tennessee Animal Care and Use Committee. Mice were euthanized by CO_2 asphyxiation.

In Vivo Hepatic TG Production

Hepatic production of VLDL-TG was measured after intraperitoneal injection of Tyloxapol (Triton WR 1339) (T0307-50G, Sigma, St. Louis, MO) (0.5mg/1g body weight) in saline on mice fasted overnight. Blood was collected from the retro-orbital plexus using heparinized microcapillary tubes (22-362-566, Fisher Scientific; Pittsburgh, PA), at 0, 1, 2, 3, and 4 hr time points after injection, and plasma was obtained by centrifugation (1,200g) at 4ºC. Plasma levels of free and total glycerol were determined using commercial colorimetric assay (TR0100, Sigma, St. Louis, MO) and plasma triglyceride concentrations were estimated by subtraction of free glycerol from total glycerol levels.

In Vivo TG Clearance

TG clearance was examined by the clearance of radiolabeled TG from a single preparation of in vivo-labeled VLDL from B6 mice, prepared as described (55). Briefly, [^{3}H] palmitic acid (P-1076, Sigma) was redissolved in saline containing 4mg/ml bovine serum albumin (690-A, Sigma) to a final concentration of 1mCi/ml. Twenty C57BL/6J (B6) mice were fasted overnight and injected intravenously through the tail vain with a bolus of [^{3}H] palmitic acid (100 µl per mouse). Mice were then killed 25 minutes after injection, and blood was collected via cardiac

puncture. Plasma was obtained by centrifugation (1,200g) at 4°C. Radiolabeled VLDL for use in the clearance study was isolated using a solution of 15.3% NaCl and 35.4% KBr (final concentration 0.65% and 1.52%, respectively) in 0.9% NaCl with a density < 1.019. Plasma (2.4 ml) was added on top of the NaCl-KBr solution (9.6 ml) and ultracentrifuged 16 hours at 40,000 x g at 4ºC (56). The tube was sliced using tube slicer (303811, Beckman) (57), and VLDL was withdrawn at 1.5 cm from the top portion using a pipette. Overnight fasted TH and B6 male mice were injected intravenously through the tail vain with 63,418 dpm of radiolabeled VLDL-TG. Blood was collected from the retro-orbital plexus using heparinized microcapillary tubes, at 5, 10, 15, and 20 minute (min) time points after injection. Plasma was obtained by centrifugation (1,200g) at 4°C. Ten µl of plasma was dissolved in 4 ml of SOLVABLE (6NE9100 Perkin Elmer, Wellesley, MA) and the radioactivity was counted in a scintillation counter (LS3801, Beckman, Fullerton, CA). The rate of clearance of VLDL-TG was determined by the disappearance of tracer, assuming the value obtained at 0 min to be 100% of the injected dose (55).

Northern Blot Analysis

Total RNA was extracted from the liver tissue of B6 and TH male mice using a RNeasy Midi Kit (75142, Quiagen, Valencia, CA). The RNA was size fractionated on a 1% agarose/2.2M formaldehyde gel, transferred by capillary action to Hybond N^+ (RPN303B, Amersham, Piscataway, NJ), and hybridized with random primed (RPN1633, Amersham) α-^{32}P-labeled apolipoprotein C-III (Apo C-III) cDNA probe. The probe was obtained by reverse transcription-polymerase chain reaction (RT-PCR) using the primers (forward: 5′-AACAAGCCTCCAAGACGGTC-3′, reverse: 5′-GGTCCTCAGGGTTAGAATCC-3′) derived from the mouse Apo C-III cDNA. The blots were washed in 2 X SSC/0.1% SDS and in 0.5 X SSC/0.1% SDS at 65ºC for 20 min each and then exposed to X-ray film at –80ºC. Quantification is conducted using ImageJ processing (JAVA).

Real Time RT-PCR

Quantitation of relative gene expressions of lipoprotein lipase (LPL) was performed by the real-time quantitative PCR using the ABI PRISM 7300 Sequence Detection System (4345250,

Applied Biosystems, Foster City, CA). Total RNA was extracted from the adipose tissue of B6 and TH male mice using RNeasy Lipid Tissue Midi Kit (75842, Quiagen, Valencia, CA) following the manufacture's protocol. The RNA (2 μg) was then reverse-transcribed in a total volume of 20 μl with SUPERSCRIPT RT (Gibco BRL, Carlsbad, CA) using oligo $d(T)_{12-18}$ as a primer following the manufacturer's instructions. Reference cDNA was synthesized using pooled RNA (total 2 μg) collected from all the samples including B6 (n=3) and TH (n=3). The primers used for the real-time PCR were proprietary for mouse LPL and mouse 18S (PPM04353A-200 and PPM57735A-200, respectively, SuperArray, Frederick, MD). Amplification of mouse 18S was performed to standardize the quantification of target cDNA. Briefly, 0.2, 0.04, 0.008, and 0.0016 μl of the reference cDNA were amplified for LPL and 18S to create a standard curve. Likewise, 0.04 μl of cDNA were amplified in all isolated mouse adipose tissue samples. PCR reactions were performed in a 25-μl volume with 0.4 μM primers and RT² Real-Time™ SYBR Green/ROX PCR master mix (PA-012, SuperArray, Frederick, MD). Amplification was achieved by denaturation (melting) at 95ºC for 30 sec, followed by 55ºC for 30 sec (annealing), and elongation at 72ºC for 35 sec. These steps were repeated for 39 cycles. After 39 cycles, amplification continued at 72ºC for 5 min. A dissociation step was added at 95ºC for 15 sec and at 60ºC for 30 sec to make sure that nothing other than the gene of interest was amplified during the reaction. After the standard curves were calculated, the input amounts of cDNA of the unknown samples were calculated for LPL and 18S. After the input amount of the probe sample was normalized to the 18S expression, the relative amount of the expressed RNA species in each unknown sample was calculated.

Bezafibrate Treatment

Diets and body and fat pad weights: At 6 weeks of age, mice were fed customized bezafibrate (B7273, Sigma) (1.5 g/kg of diet) containing or regular chow diet for 15 weeks. Body weights were measured weekly. At the end of the study, mice were killed, and five white (including inguinal, epididymal, mesenteric, retroperitoneal (including perirenal), and subscapular)

and brown fat pads were dissected and weighed to measure adiposity. Carcass weights (body weight without the white fat pads) were then measured.

Plasma Glucose, Insulin, and TG levels: Blood was drawn between 7:30 and 10:30 AM from the retro-orbital plexus using heparinized microcapillary tubes, and plasma was obtained by centrifugation (1,200g) at 4°C. Plasma TG (TR0100, Sigma) and glucose (TR15221, Thermo Electron, Louisville, CO) levels were determined using commercial colorimetric kits. Plasma insulin levels were determined using RIA kits (RI-13K, Linco Research, St. Charles, MO).

Intraperitoneal Glucose Tolerance Test: Mice were fasted overnight and then injected intraperitoneally with glucose (1mg/g body weight) in saline. Blood was drawn from the retro-orbital plexus using heparinized microcapillary tubes at 0, 30, 60, and 120 min after injection. Plasma was obtained by centrifugation (1,200g) at 4°C. Plasma glucose levels were then determined using a commercial colorimetric kit as described above.

Tissue Glucose Uptake: Overnight fasted mice were injected intravenously through the tail vein with a bolus of 2-Deoxy-D-Glucose 1,2-^{3}H(N) (2-DG) (D4539, Sigma) (10μCi)/mouse (58) in saline either with or without insulin (I-5523, Sigma) (1U/ml). The mice were euthanized by CO_2 asphyxiation 30 min after injection. Epididymal fat pads and soleus muscle were then collected, washed, blot dried, and weighed, and dissolved in 1M-NaOH solution at 60°C (fat pads) or in SOLVABLE (soleus muscle) (6NE9100, Perkin Elmer). The incorporated radioactivity was counted in a scintillation counter (LS3801, Beckman). The 2-DG uptake was expressed as the counts per minute divided by tissue weight (58).

Statistical Analysis

Data analysis was conducted by ANOVA with StatView 5.0 (Abacus Concepts, Berkeley, CA). All data were presented as mean ± SEM.

III. RESULTS

Hepatic VLDL-TG Production

To evaluate hepatic VLDL production, overnight fasted B6 and TH mice were injected with Triton WR 1339 to block LPL-mediated TG hydrolysis, and the accumulation of TG (VLDL-TG) in plasma was monitored over time. As shown in figure 1, basal TG levels were significantly different between TH and B6 mice, but maximum secretion was not.

VLDL-TG Clearance

To determine whether HTG in TH mice is associated with TG removal, we examined the plasma clearance of [^{3}H] TG-labeled VLDL obtained from B6 control mice. The mean percentages of residual [^{3}H] TG-labeled VLDL in the plasma are depicted in figure 2. TH mice showed a significantly increased residual percentage of injected [^{3}H] TG-labeled VLDL at all sampling times compared to B6 mice, indicating slower clearance rate in TH mice than in B6 mice.

Gene Expression Levels of Apo C-III and LPL

Consistent with studies demonstrating that over-expression of Apo C-III is positively associated with pronounced HTG (59, 60), the gene expression level of Apo C-III was higher in TH mice compared to B6 mice as shown in the autoradiographs (figure 3). There was no difference in gene expression of LPL between TH and B6 mice (figure 4).

Effects of Bezafibrate Treatment

Body and fat pad weights: Fat pads and carcass weights were significantly higher in TH mice compared to B6 mice on chow (figures 5 & 6). BF treatment did not change adiposity in these mice (figures 5 & 6).

Plasma Levels of TG, Glucose, and Insulin: At 6 week of age, the basal plasma TG levels were significantly higher in TH mice compared to B6 mice (figure 7). BF treatment markedly lowered plasma TG levels both in TH and B6 mice (figure 7). Plasma glucose levels of both TH and B6 mice were similar throughout the study showing no significant effect of BF (figure 8). The basal plasma insulin levels in TH mice were significantly higher than those in B6 mice at 6 weeks of age, and the hyperinsulinemia was maintained throughout the study period in TH mice (figure 9).

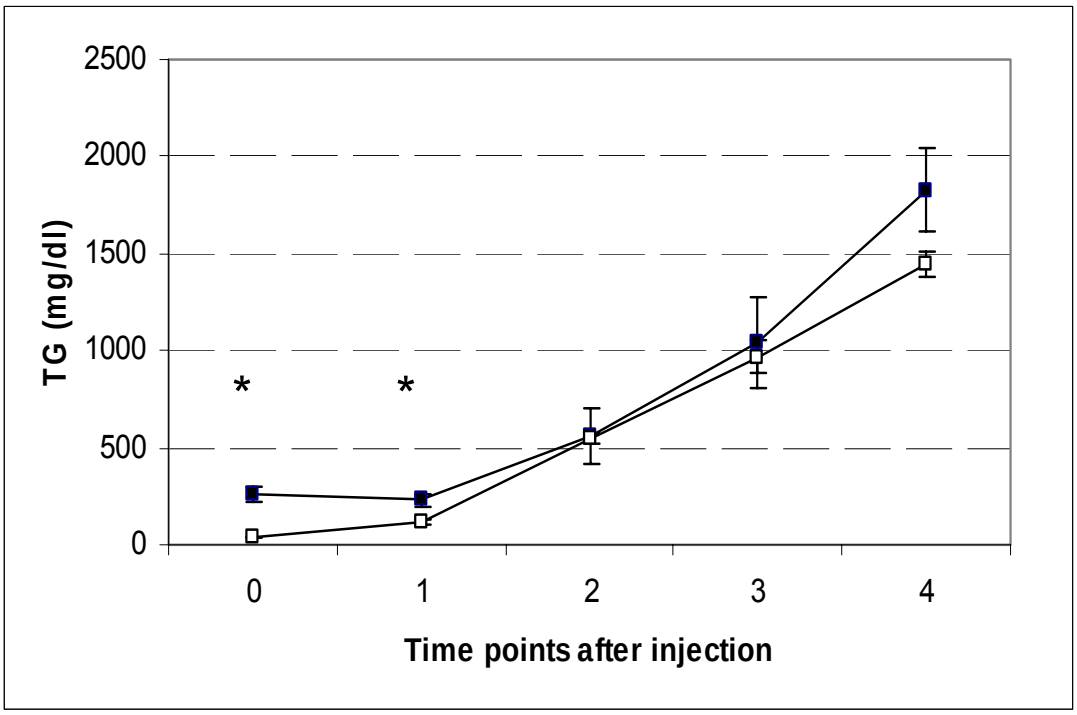

Figure 1. Hepatic VLDL TG production in B6 and TH mice. Triton WR 1339 (0.5mg/1g body weight) was injected into fasted B6 (open squares) and TH (filled squares) at 8 wks of age. Plasma TG levels were determined at the indicated time points and corrected for the TG level at the time of Triton injection (0 min). The values represent means ± SEM of 5 mice/group. *p < .006 vs B6

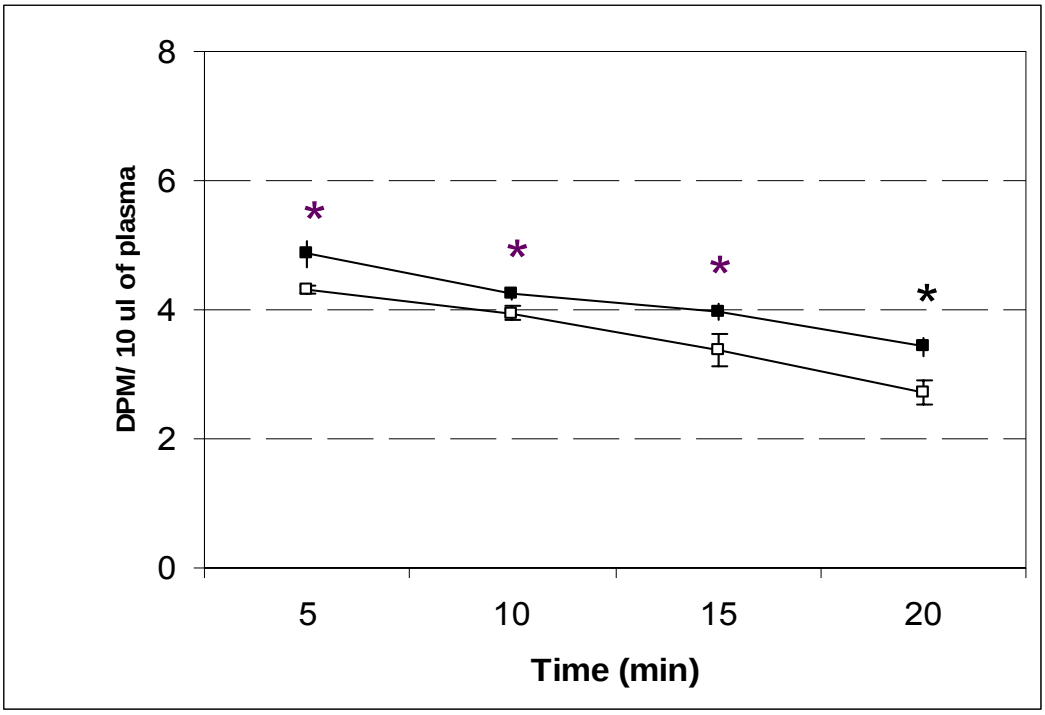

Figure 2. Clearance of VLDL (d < 1.019) in B6 and TH mice. VLDL labeled on its TG moiety was obtained 25 min after injecting B6 mice with [3H] palmitate. The isolated labeled VLDL was then injected (63,418 dpm/ mouse) into B6 and TH mice at 12 weeks of age. At the indicated times, blood (<50 μl) were taken, and radioactivity in plasma of 10 μl was counted. The plasma decay of the label was more rapid in B6 (open squares) than in TH (closed squares) mice. The values represent means ± SEM of 9 mice per group. *p<0.05 vs. B6 at the time point.

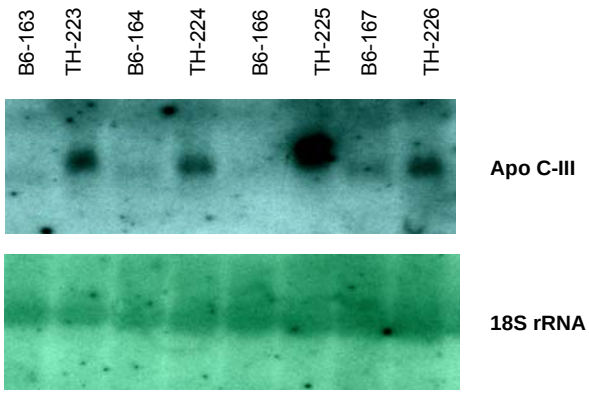

Figure 3. Autoradiograph of Northern blot analysis for Apo C-III gene in the liver from B6 (n=4) and TH (n=4) mice (males, 12 weeks). Total RNA was loaded for each sample. Northern blot hybridization was carried out with a mouse Apo C-III cDNA probe and equal loading was verified by hybridization to an 18S rRNA probe.

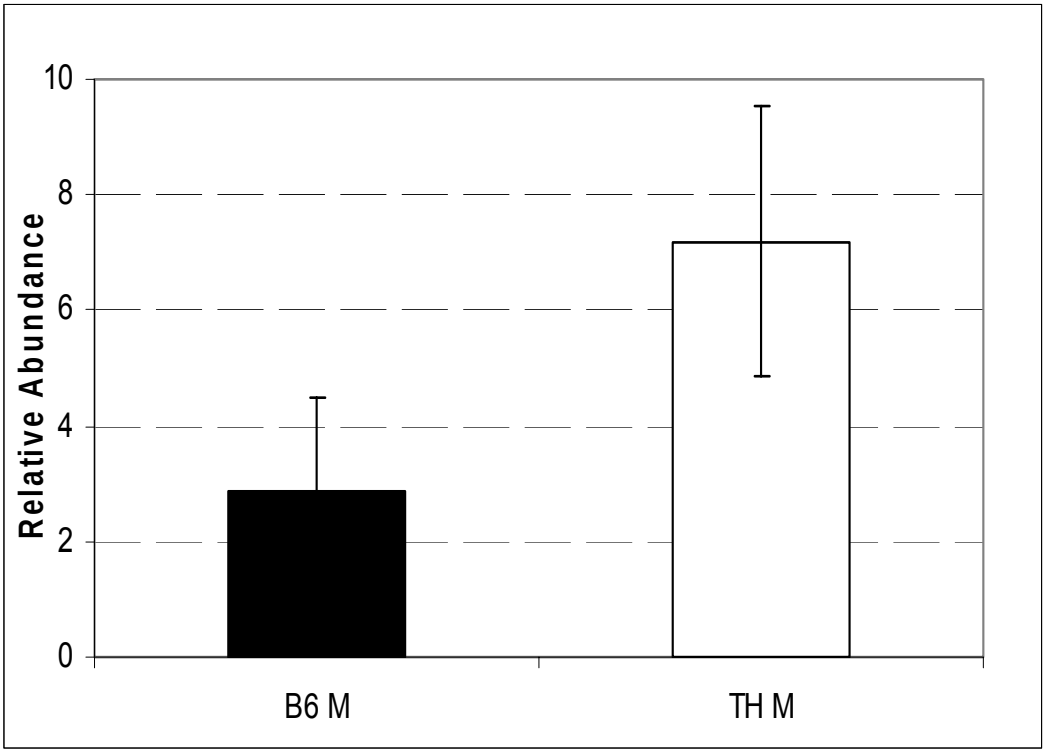

Figure 4. Lipoprotein lipase mRNA levels by real-time RT-PCR analysis in B6 (n=3) and TH (n=3) mice (males, 12 weeks). Values are displayed as relative abundance after normalization to 18S rRNA expression levels in the same sample.

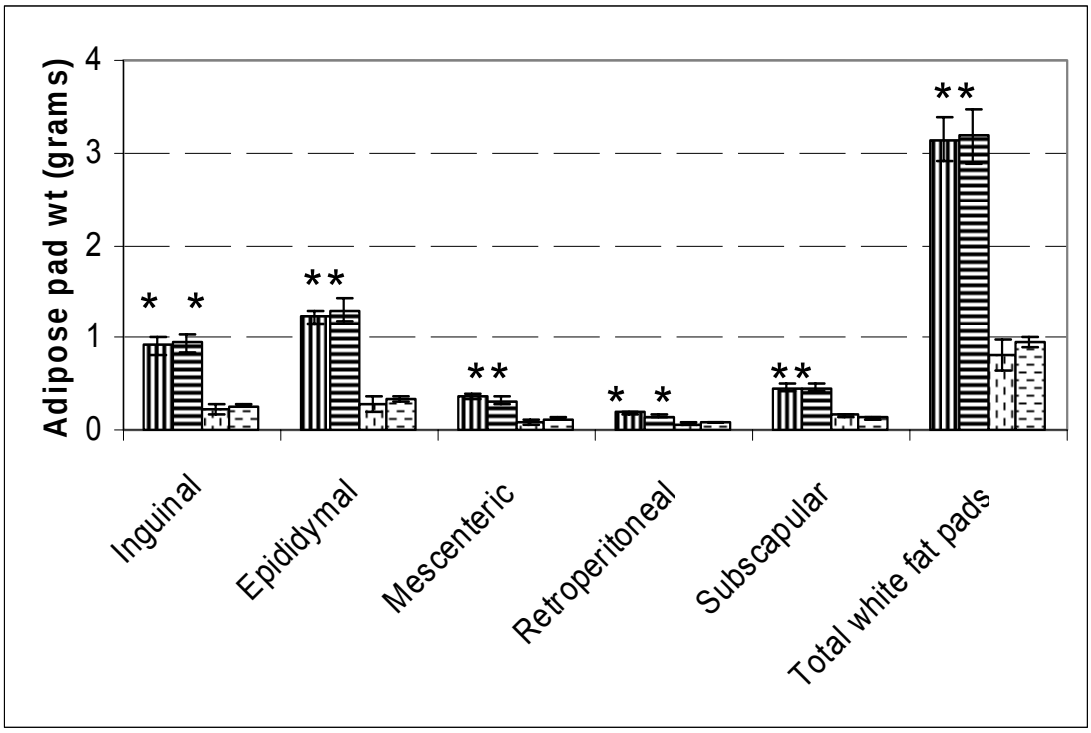

Figure 5. Fat pad weights in TH and B6 mice fed chow and bezafibrate-treated (BF) diets for 15 wk beginning at 6 wk of age (males). At the end of the study, mice were euthanized, five white fat pads [inguinal, epididymal, mesenteric, retroperitoneal (including perirenal), and subscapular] were dissected and weighed. The first two bars in the group represent TH mice and the last two bars represent B6. Vertical lines represent chow and horizontal lines BF diets, respectively (males, n = 3-11 for each group). Values are expressed as means ± SEM. *$p<0.05$ vs. B6 mice. There was no significant diet effect.

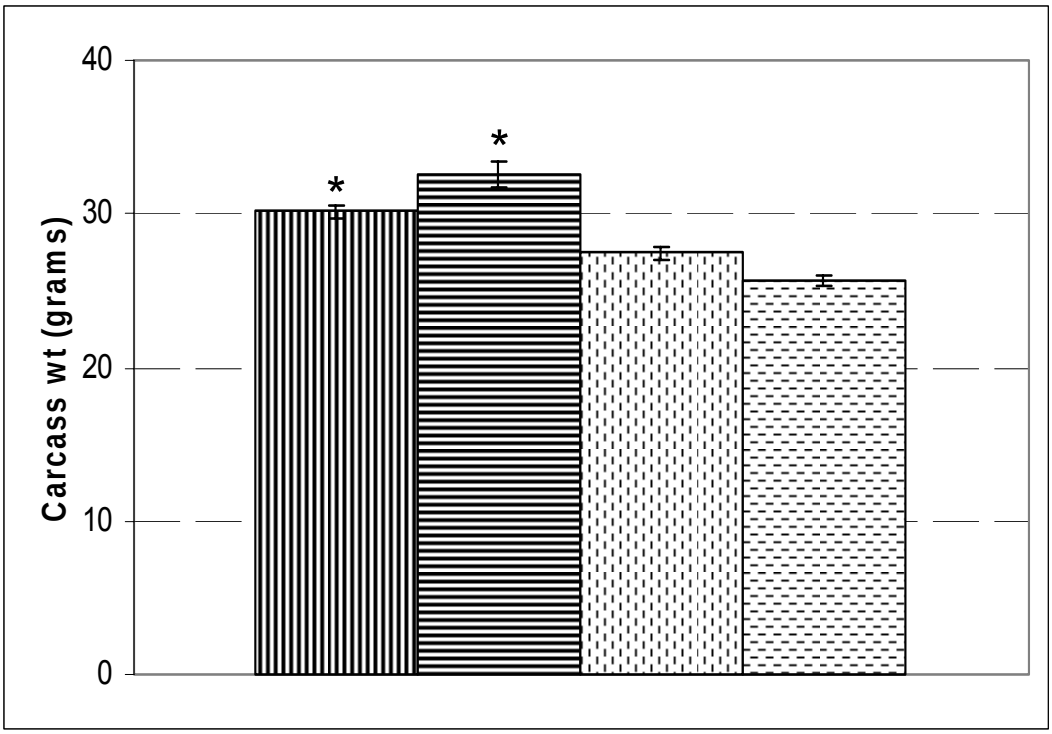

Figure 6. Carcass weights (body weight without the five white fat pads) in TH and B6 mice fed chow and bezafibrate-treated (BF) diets for 15 wk beginning at 6 wk of age (males). The first two bars in the group represent TH mice and the last two bars represent B6. Vertical lines represent chow diet and horizontal lines BF diets, respectively. *p <0.05 vs. B6 mice. There was no significant diet effect.

A.

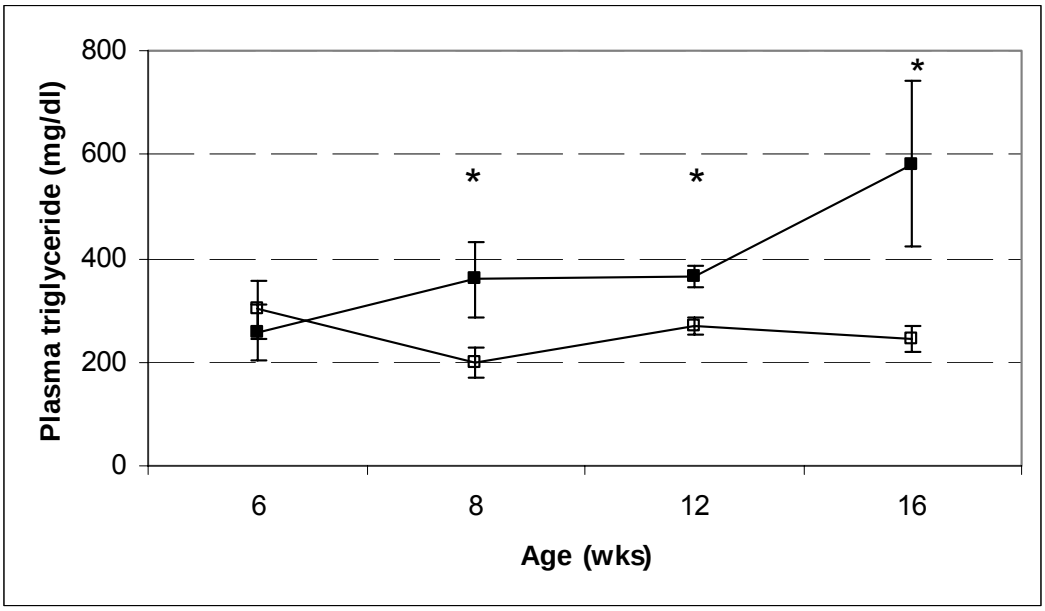

B.

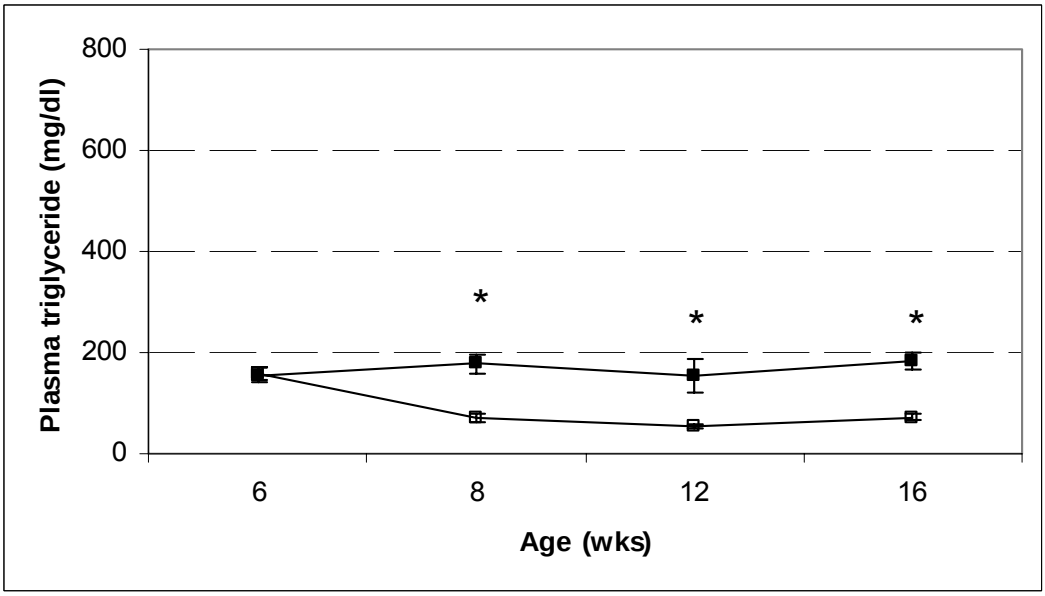

Figure 7. Changes in plasma triglyceride levels in TH (a) and B6 (b) mice fed chow and bezafibrate-treated (BF) diets for 15 wk beginning at 6 wk of age (males). Blood was drawn between 7:30 and 10:30 AM from the retroorbital plexus using heparinized microcapillary tubes, and plasma was obtained by centrifugation (1,200 *g*) at 4°C. Plasma TG levels were then determined using a commercial colormetric kit. Open and filled symbols represent BF and chow diets, respectively (non-fasting, n = 6-15 for each group). Values are expressed as means ± SEM. *$p < 0.05$ vs. chow.

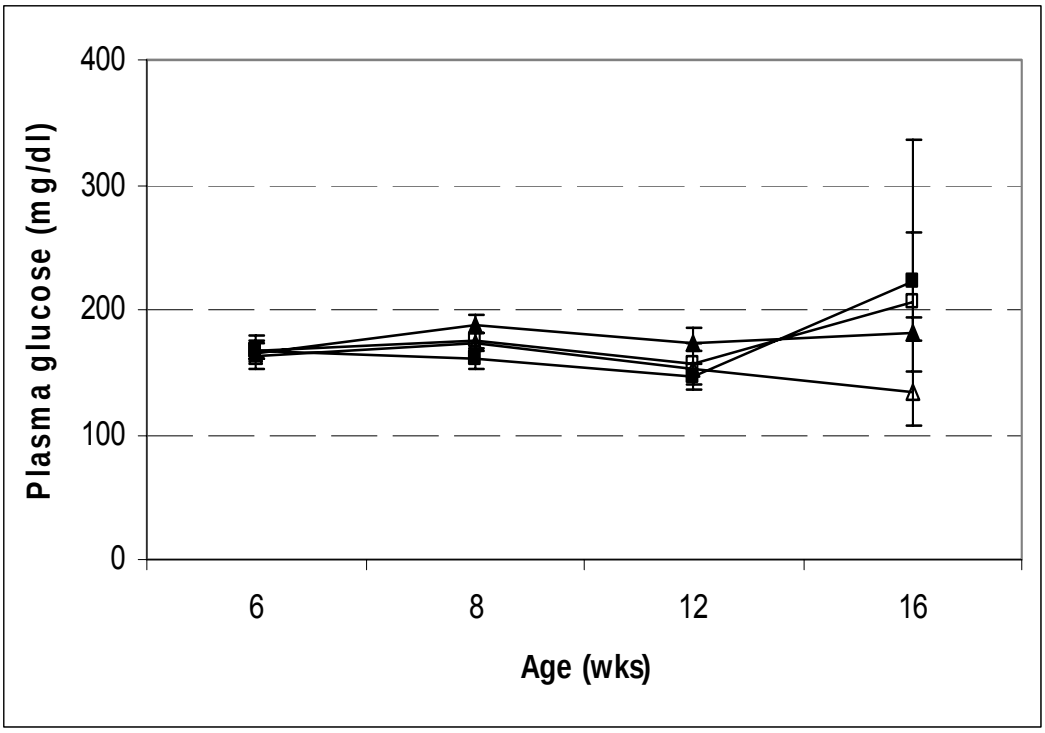

Figure 8. Changes in plasma glucose levels in TH and B6 mice fed chow and bezafibrate-treated (BF) diets for 15 wk beginning at 6 wk of age (males). Blood was drawn between 7:30 and 10:30 AM from the retroorbital plexus using heparinized microcapillary tubes, and plasma was obtained by centrifugation (1,200 *g*) at 4°C. Plasma glucose levels were then determined using a commercial colormetric kit. Squares and triangles represent TH and B6, respectively. Open and filled symbols represent BF and chow diets, respectively (non-fasting, n = 6-15 for each group).

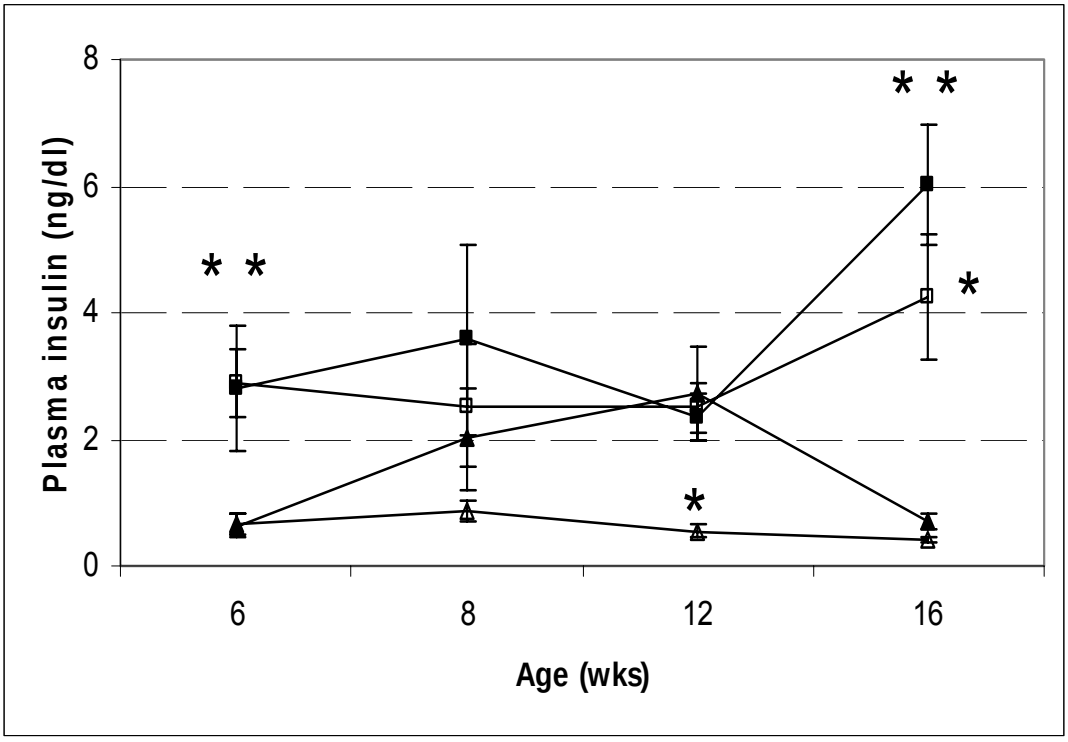

Figure 9. Changes in plasma insulin levels in TH and B6 mice fed chow and bezafibrate-treated (BF) diets for 15 wk beginning at 6 wk of age (males). Blood was drawn between 7:30 and 10:30 AM from the retroorbital plexus using heparinized microcapillary tubes, and plasma was obtained by centrifugation (1,200 *g*) at 4°C. Plasma insulin levels were then determined using a RIA kit. Squares and triangles represent TH and B6, respectively. Open and filled symbols represent BF and chow diets, respectively (male, non-fasting, n = 3-12 for each group). Values are expressed as means ± SEM **p <0.01 vs B6; *p<0.05 vs. chow.

BF treatment slightly, but significantly, decreased plasma insulin levels in TH mice at 16 weeks of age, 10 weeks on the treatment (figure 9).

Intraperitoneal Glucose Tolerance Test: TH mice exhibited impaired glucose tolerance compared to B6 mice (figure 10). BF treatment did not improve glucose tolerance in TH mice (figure 10).

Glucose uptake: The effect of BF treatment on glucose uptake, the first step of glucose metabolism in the body, was tested *in vivo* in the insulin sensitive soleus muscle and epididymal fat of TH mice, using 2-DG (a glucose analogue that is taken up by cells but not metabolized). BF treatment did not improve 2-DG uptake in either soleus muscle or epididymal fat pad in TH mice (figure 11 and 12).

IV. DISCUSSION

HTG, the most commonly seen lipid abnormality in T2DM, can result from an increased hepatic production of VLDL-TG that leads to increased VLDL-TG secretion, or a delayed catabolism of plasma TG, or both (61). In this study, we have found a marked reduction in VLDL-TG clearance rate in TH mice compared to B6 mice without a significant difference in hepatic VLDL-TG production (figures 1 and 2). There was also evidence that the Apo C-III gene expression was upregulated in the liver of TH mice (figure 3). Further, our study demonstrated that lowering plasma TG with BF treatment failed to improve glucose metabolism in TH mice (figures 5-12).

Like in TH mice, the HTG in streptozocin-induced diabetic rats is due to reduced VLDL-TG catabolism while the secretion rate of TG is normal (62, 63). This demonstrates that HTG is attributable to a defect of TG clearance either in insulin resistance or deficiency.

The molecular mechanism of HTG, however, remains unclear. Various research groups have investigated the roles of apolipoproteins in the regulation of TG metabolism through in vitro and in vivo studies. An increasing body of evidence has implicated Apo C-III as a contributing factor for the development of HTG in humans and animals.

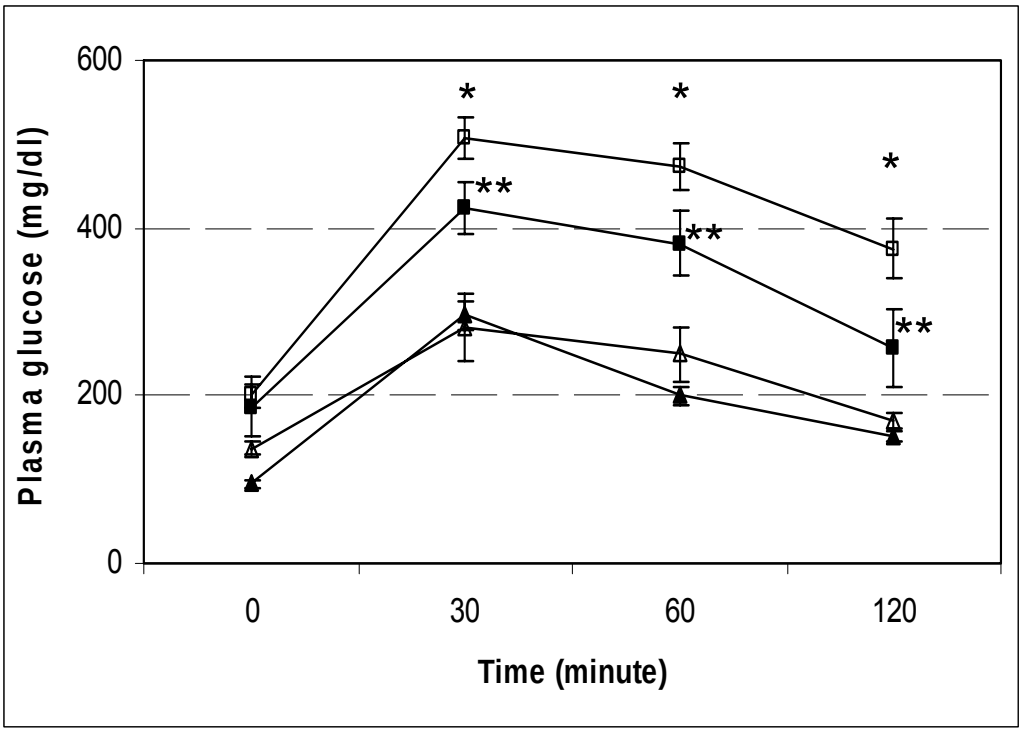

Figure 10. Glucose tolerance test in TH and B6 mice fed chow and bezafibrate-treated (BF) diets for 15 wk beginning at 6 wk of age (males, 17 wks of age). Mice were fasted overnight and injected intraperitoneally with glucose (1mg/g body weight) in saline. Blood was collected via the retroorbital plexus using a heparinized microcapillary tube at 0, 30, 60, and 120 min after injection. Plasma glucose levels were then determined using a commercial colorimetric kit. Squares and triangles represent TH and B6, respectively. Open and filled symbols represent BF and chow diets, respectively (n = 5-7 for each group). Values are expressed as means ± SEM. *p <0.05 vs. TH on chow; **p <0.01 vs. B6 on both diets.

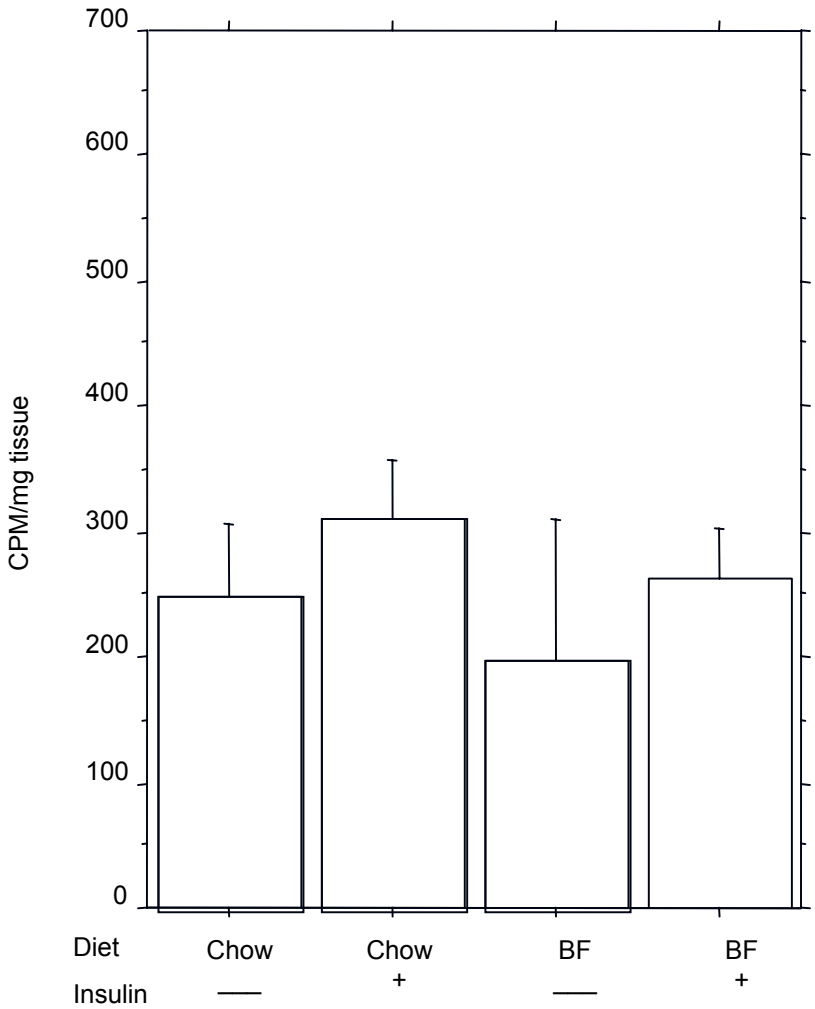

Figure 11. In vivo 2-deoxy-D-glucose 1, 2-[3H] (N) (2-DG) uptake in soleus muscle in TH mice fed chow and bezafibrate-treated (BF) diets for 15 wk beginning at 6 wk of age (males, 18 wk, n = 2- 4 for each group). Mice were fasted overnight and injected with a bolus of 2-DG in saline without (W/O) or with insulin and tissue was harvested 30 min after the injection.
2-DG uptake is expressed as counts per minute (CPM) normalized by mg tissue.

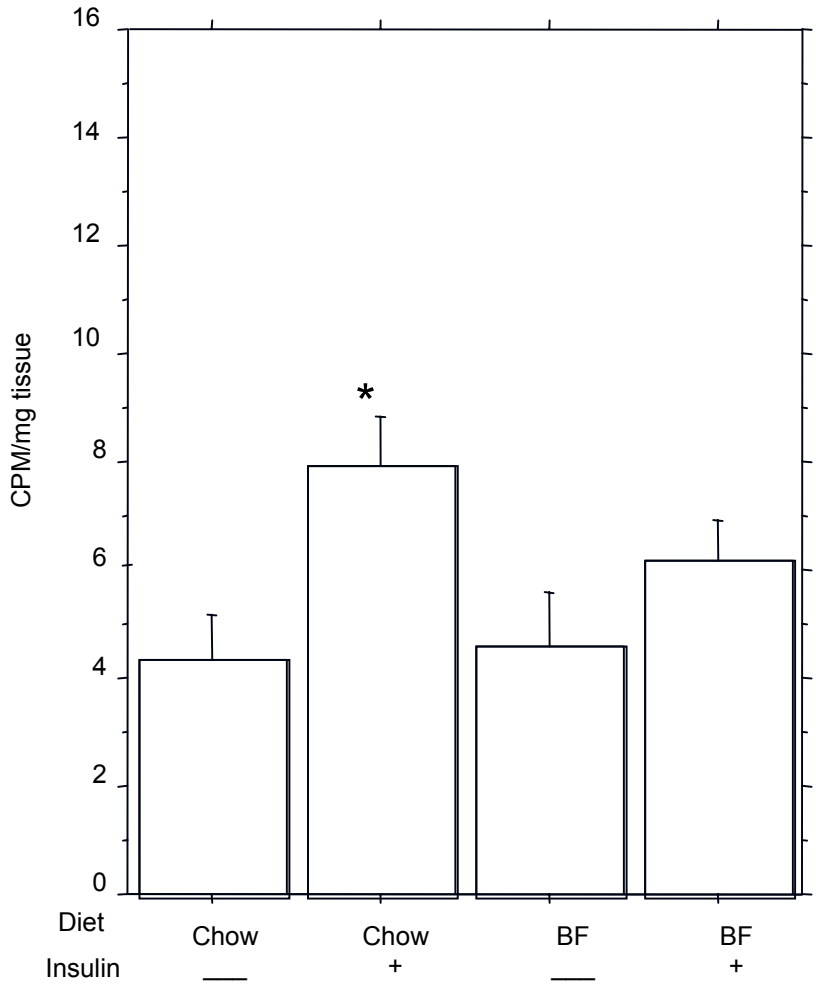

Figure 12. In vivo 2-deoxy-D-glucose 1, 2-[3H] (N) (2-DG) uptake in epididymal fat in TH mice fed chow and bezafibrate-treated (BF) diets for 15 wk beginning at 6 wk of age (males, 18 wk, n = 4 for each group). Mice were fasted overnight and injected with a bolus of 2-DG in saline without (W/O) or with insulin and tissue was harvested 30 min after the injection. Epididymal fat pads were collected, washed, blot dried, weighed, and dissolved in 1 M NaOH at 60°C. Incorporated radioactivity was counted in a scintillation counter. 2-DG uptake is expressed as counts per minute (CPM) normalized by mg tissue . *p <0.05 vs. chow W/O insulin.

Apo C-III, mainly synthesized in the liver, is a 79 amino acid protein with a molecular mass of 8.8 kDa and becomes a component of chylomicrons (CM), VLDL and HDL (64). It has been demonstrated that elevated Apo C-III levels are positively associated with HTG in humans (65, 66). In addition, over-expression of the human and mouse Apo C-III gene in transgenic mice results in HTG, the severity of which is associated with the levels of plasma Apo C-III (46, 67). Apo CIII deficient mice, on the other hand, develop hypotriglyceridemia (47).

The causal link between overexpression of Apo C-III and HTG has been demonstrated by impaired clearance of VLDL-TG. Apo C-III transgenic mice had impaired clearance of VLDL-TG (67), whereas Apo C-III null mice exhibited an increased catabolic rate of VLDL-TG (44). The hypotriglyceridemia shown in Apo C-III null mice is primarily due to an increased hydrolysis of VLDL-TG via LPL (44), (68). LPL, a 52-kD protein, is a rate-limiting enzyme for TG hydrolysis in CM and VLDL (69-71). It has been known that Apo C-III inhibits LPL function, although the mechanism is unknown. On the basis of in vitro studies, the proposed mechanism by which Apo C-III inhibits LPL activity includes either a direct interaction of Apo C-III with LPL (70), or a hampered binding of the Apo C-III-enriched lipoprotein particles to heparan sulfate proteoglycan-LPL matrix on the surface of endothelial cells (72). However, in vivo evidence has demonstrated that Apo C-III inhibits the interaction of VLDL with heparan sulfate proteoglycan rather than acting as a direct inhibitor of LPL (67, 68, 73). In the present study, we did not test clearance of VLDL particles from TH mice. Therefore, it remains unknown whether the slowed clearance of VLDL from TH mice is attributable to an altered composition of VLDL particles, or to a problem in VLDL-TG hydrolysis system, because it is possible that a rapid exchange of apolipoproteins occurs between injected VLDL derived from the control B6 mice and the recipient TH lipoproteins during the VLDL clearance test. Although there was no evidence of downregulation of LPL mRNA in TH mice, LPL activity study is required to address this question. Also, the clearance test using VLDL derived from TH mice is required to be conducted to understand the effect of VLDL component on the hydrolysis of TG.

It is well known that diabetes is associated with a reduction of LPL activity at the posttranscriptional level (38, 73, 74). Therefore, it is possible that LPL activity may be reduced in TH mice due to insulin resistance, and overproduction of Apo C-III causes further functional deficiency of LPL in TH mice.

Several studies have implicated that dyslipidemia can be responsible for altered insulin action and glucose metabolism. Roden et al (1996) demonstrated that an intravenous infusion of a TG emulsion into healthy individuals decreased muscle glycogen synthesis and the rate of whole-body glucose uptake (75). Dresner et al. (1999) also demonstrated that lipid infusion abolished insulin signaling (34). Normalization of TG levels lowered fasting plasma glucose levels more than 3 times and improved insulin sensitivity in subjects with extreme HTG and overt diabetes (76). Previously, we have found that insulin resistance is profoundly associated with HTG in male TH mice (unpublished data). However, it is unknown whether the HTG is the primary defect for the reduced insulin sensitivity or the secondary to the insulin resistance in TH mice. Therefore, in the present study we examined the effect of a lipid lowering drug bezafibrate on insulin sensitivity in TH mice. Bezafibrate is known to selectively decrease plasma TG levels without affecting blood glucose levels (77).

Bezafibrate treatment significantly lowered the plasma TG levels both in TH and B6 mice until the end of the study period. Despite lowering plasma TG levels, bezafibrate treatment did not improve glucose tolerance and uptake in TH mice, although it slightly ameliorated hyperinsulinemia at the late stage of the study. Glucose tolerance and insulin stimulated 2-DG uptake in epididymal fat even worsened with bezafibare treatment in TH mice. Presently, we have no explanation for these changes. Collectively, these findings suggest that the HTG may not be responsible for the altered glucose metabolism in TH mice.

A lack of bezafibrate effect on improving glucose metabolism was also shown in Zucker Diabetic Fatty (ZDF) rats (77). Also, Jia et al (29) only found a minor effect of bezafibrate on insulin sensitivity in the Otsuka Long-Evans Tokushima Fatty (OLETF) rats. In contrast, BF treatment significantly decreased fasting serum insulin, glucose and TG levels and improved

insulin sensitivity in non-obese Japanese type 2 diabetic subjects (31). Also, Matsui et al have reported that bezafibrate treatment improves insulin sensitivity in Sprague-Dawley rats fed high-fructose and lard diets (78). These contradictory effects of bezafibrate on insulin sensitivity and glucose metabolism might be associated with differences in species, doses and durations used in different studies.

In summary, the HTG appears to be due to a defect in TRL-TG clearance in TH mice, and overproduction of Apo C-III may be in part involved in the pathogenesis. The HTG is not likely responsible for the impaired insulin action in TH mice, but insulin resistance may be the primary defect. These results shed light on the mechanism underlying the HTG in obese type 2 diabetic TH mice, which may contribute to understanding the pathophysiology of diabetic HTG in humans and provide biochemical targets for the intervention.

CHAPTER 4: CONCLUSIONS AND FUTURE DIRECTIONS

It has long been recognized that diabetes is a disorder not only of carbohydrate metabolism, but also of lipid metabolism. HTG is the dominant dyslipidemia observed in diabetic patients, especially with T2DM, and is known to be a strong risk factor for coronary heart disease (CHD) in T2DM. However, the molecular mechanism underlying the diabetic HTG is largely unknown. In the present study, we have found that obese type 2 diabetic TH mice have defective VLDL-TG clearance. In support of the slowed VLDL-TG clearance rate, we also found evidence of hepatic over-expression of the *Apo C*-III gene, known as an inhibitor of LPL, in TH mice. The activity of LPL in TH mice requires to be determined. In addition to Apo C-III, other apolipoproteins including Apo C-II and Apo A-V are known to be important regulators for plasma TG metabolism. Apo C-II and Apo A-V are both specifically expressed in the liver and augments lipolysis of plasma TG (79) (40). Studying abnormalities in molecular properties and biological functions of these apolipoproteins may identify a determinant of diabetic HTG in TH mice.

Further, our long term study includes genetic characterization of HTG in TH mice. The importance of genetic controls in lipid metabolism has been demonstrated through epidemiological studies illustrating that 30 to 45% of the phenotypic variance for lipid and lipoprotein phenotypes is accounted by genes whereas environmental factors account for less than 15% of the variance (80). Therefore, genetic dissection of susceptibility genes accounting for the HTG in TH mice will provide important information for understanding the underlying molecular mechanism of HTG in this model.

Knowing the pathophysiological mechanism and genes responsible for the HTG in TH mice will provide ready targets for lipid lowering therapy, ultimately preventing CHD, in T2DM patients. This will also provide a new mouse model for T2DM with dyslipidemia that will be useful for understanding relationship between lipid metabolism and glucose metabolism.

REFERENCES

1. Hiukka A, Fruchart-Najib J, Leinonen E, Hilden H, Fruchart JC, Taskinen MR. Alterations of lipids and apolipoprotein CIII in very low density lipoprotein subspecies in type 2 diabetes. Diabetologia. 2005 Jun;48:1207-15.
2. National Diabetes Information Clearinghouse. National Diabetes Statistics. 2006 [cited 2005 January]; Available from: http://diabetes.niddk.nih.gov/dm/pubs/statistics/#14
3. Center for Disease Control and Prevention. "Diabetes: Disabling, Deadly, and on the Rise." [cited 2005 May]; Available from: http://www.cdc.gov/nccdphp/publications/aag/ddt.htm
4. Groop LC, Tuomi T. Non-insulin-dependent diabetes mellitus--a collision between thrifty genes and an affluent society. Ann Med. 1997 Feb;29:37-53.
5. Koopman RJ. Changes in Age at Diagnosis of Type 2 Diabetes Mellitus in the United States, 1988 to 2000 Annals of Family Medicine (2005);3:60-6.
6. Center for Disease Control and Prevention, Data & Trends. National Diabetes Surveillance System. [cited 2006 January]; Available from: http://www.cdc.gov/diabetes/statistics/prev/national/figpersons.htm
7. Krauss RM. Lipids and Lipoproteins in Patients with Type 2 Diabetes. Diabetes Care 2004;27:1496-504.
8. Beck-Nielsen H, Groop LC. Metabolic and genetic characterization of prediabetic states. Sequence of events leading to non-insulin-dependent diabetes mellitus. J Clin Invest. 1994 Nov;94:1714-21.
9. Alcolado, JC and DA Rees. Animal models of diabetes mellitus. Diabetic Medicine. 2005 March 24;22:359–70.
10. Kim, JH. In Genomics and Proteomics in Nutrition.
New York: Marcel Dekker; 2004.
11. Leiter EH, Reifsnyder PC. Differential levels of diabetogenic stress in two new mouse models of obesity and type 2 diabetes. Diabetes. 2004 Feb;53 Suppl 1:S4-11.
12. Kim JH. Genetic Analysis of a New Mouse Model for Non-Insulin Dependent Diabetes. Genomics 2001;74:273-86.
13. Center for Disease Control and Prevention, National Center for Health Statistics. Deaths/Mortality. [cited (2005) November 9]; Available from: http://www.cdc.gov/nchs/fastats/deaths.htm
14. Clark C. How should we respond to the worldwide diabetes epidemic? Diabetes Care. 1998;21:475-6.
15. Burke JW, K, Gaskill, S. Hazuda, H, Haffner, S, Stern M. Rapid rise in the incidence of type 2 diabetes from 1987 to 1996: Results from the San Antonio Heart Study. Archives of Internal Medicine. 1999;159:1450-7.
16. National Center for Health Statistic. "Prevalence of Overweight and Obesity Among Adults: United States, 1999-2002." [cited 2004 December 16]; Available from: http://www.cdc.gov/nchs/products/pubs/pubd/hestats/obese/obse99.htm
17. Hensrud DD. Dietary Treatment and Long-Term Weight Loss and Maintenance in Type 2 Diabetes. Obesity Research (2001);9:S348-S53.
18. Costacou T, Mayer-Davis EJ. Nutrition and prevention of type 2 diabetes. Annual Review Nutrition (2003);23:147-70.
19. Ikegami H, Fujisawa T, Ogihara T. Mouse models of type 1 and type 2 diabetes derived from the same closed colony: genetic susceptibility shared between two types of diabetes. Ilar J. 2004;45:268-77.
20. Hodge AM, Dowse GK, Zimmet PZ, Collins VR. Prevalence and secular trends in obesity in Pacific and Indian Ocean island populations. Obesity Research. 1995;3 (suppl 2):77-87S.
21. American Dietetic Association. "Diabetes & Your Weight. "What is the link between diabetes and obesity?" [cited 2005 June]; Available from: http://www.diabetes.org/weightloss-and-exercise/weightloss/diabetes.jsp
22. Chiasson J-L, Rabasa-Lhoret R. Section I: Insulin Resistance-Beta-Cell Connection in Type 2 Diabetes. Prevention of Type 2 Diabetes. Insulin Resistance and Beta-Cell Function. Diabetes 2004;53:S34-S8.

23. Grundy SM, Bryan Brewer, H, Cleeman, J, Smith S, Lenfant, C. Definition of Metabolic Syndrome. Arteriosclerosis, Thrombosis, and Vascular Biology (2004);24:e13.
24. Ferre P. The biology of peroxisome proliferator-activated receptors: relationship with lipid metabolism and insulin sensitivity. Diabetes. 2004 Feb;53 Suppl 1:S43-50.
25. Taskinen M-R. Type 2 Diabetes as a Lipid Disorder. Current Molecular Medicine (2005);5:297-30.
26. Lamarche B, Moorjani S, Cantin B, Dagenais GR, Lupien PJ, Despres JP. Associations of HDL2 and HDL3 subfractions with ischemic heart disease in men. Prospective results from the Quebec Cardiovascular Study. Arterioscler Thromb Vasc Biol. 1997 Jun;17:1098-105.
27. Hokanson JE, Austin MA. Plasma triglyceride level is a risk factor for cardiovascular disease independent of high-density lipoprotein cholesterol level: a meta-analysis of population-based prospective studies. J Cardiovasc Risk. 1996 Apr;3:213-9.
28. Kota BP, Huang TH, Roufogalis BD. An overview on biological mechanisms of PPARs. Pharmacol Res. 2005 Feb;51:85-94.
29. Jia D, Yamamoto M, Otani M, Otsuki M. Bezafibrate on lipids and glucose metabolism in obese diabetic Otsuka Long-Evans Tokushima fatty rats. Metabolism. 2004 Apr;53:405-13.
30. Staels B, Dallongeville J, Auwerx J, Schoonjans K, Leitersdorf E, Fruchart JC. Mechanism of action of fibrates on lipid and lipoprotein metabolism. Circulation. 1998 Nov 10;98:2088-93.
31. Taniguchi A, Fukushima M, Sakai M, Tokuyama K, Nagata I, Fukunaga A, Kishimoto H, Doi K, Yamashita Y, Matauura T, Kitatani N, Okumura T, Nagasaka S, Nakaishi S, Nakai Y. Effects of bezafibrate on insulin sensitivity and insulin secretion in non-obese Japanese type 2 diabetic patients. Metabolism. 2001 Apr;50:477-80.
32. Kingsbury KJ. Understanding the Essentials of Blood Lipid Metabolism. Progress in Cardiovascular Nursing. 2003;18:13-8.
33. National Diabetes Information Clearinghouse.
Insulin Resistance and Pre-Diabetes [cited 2006 February]; Available from: http://diabetes.niddk.nih.gov/dm/pubs/insulinresistance/
34. Dresner A, Laurent D, Marcucci M, Griffin ME, Dufour S, Cline GW, Slezak LA, Andersen DK, Hundal RS, Rothman DL, Petersen KF, Shulman GI. Effects of free fatty acids on glucose transport and IRS-1-associated phosphatidylinositol 3-kinase activity. J Clin Invest. 1999 Jan;103:253-9.
35. Levak-Frank S, Weinstock PH, Hayek T, Verdery R, Hofmann W, Ramakrishnan R, Sattler W, Breslow JL, Zechner R. Induced mutant mice expressing lipoprotein lipase exclusively in muscle have subnormal triglycerides yet reduced high density lipoprotein cholesterol levels in plasma. J Biol Chem. 1997 Jul 4;272:17182-90.
36. Koike T, Liang J, Wang X, Ichikawa T, Shiomi M, Liu G, Sun H, Kitajima S, Morimoto M, Watanabe T, Yamada N, Fan, J. Overexpression of lipoprotein lipase in transgenic Watanabe heritable hyperlipidemic rabbits improves hyperlipidemia and obesity. J Biol Chem. 2004 Feb 27;279:7521-9.
37. Nierman MC, Rip J, Twisk J, Meulenberg JJ, Kastelein JJ, Stroes ES, Kuivenhoven JA. Gene therapy for genetic lipoprotein lipase deficiency: from promise to practice. Neth J Med. 2005 Jan;63:14-9.
38. Tavangar K, Murata Y, Pedersen ME, Goers JF, Hoffman AR, Kraemer FB. Regulation of lipoprotein lipase in the diabetic rat. J Clin Invest. 1992 Nov;90:1672-8.
39. Medline Plus. Medical Dictionary.
40. Merkel M, Heeren J. Give me A5 for lipoprotein hydrolysis! J Clin Invest. 2005 Oct;115:2694-6.
41. Boguski MS, Birkenmeier EH, Elshourbagy NA, Taylor JM, Gordon JI. Evolution of the apolipoproteins. Structure of the rat apo-A-IV gene and its relationship to the human genes for apo-A-I, C-III, and E. J Biol Chem. 1986 May 15;261:6398-407.
42. Zilversmit DB. Atherogenic nature of triglycerides, postprandial lipidemia, and triglyceride-rich remnant lipoproteins. Clin Chem. 1995 Jan;41:153-8.

43. Lusis AJ, Fogelman AM, Fonarow GC. Genetic basis of atherosclerosis: part II: clinical implications. Circulation. 2004 Oct 5;110:2066-71.
44. Jong MC, Rensen PC, Dahlmans VE, van der Boom H, van Berkel TJ, Havekes LM. Apolipoprotein C-III deficiency accelerates triglyceride hydrolysis by lipoprotein lipase in wild-type and apoE knockout mice. J Lipid Res. 2001 Oct;42:1578-85.
45. Conde-Knape K, Okada K, Ramakrishnan R, Shachter NS. Overexpression of apoC-III produces lesser hypertriglyceridemia in apoB-48-only gene-targeted mice than in apoB-100-only mice. J Lipid Res. 2004 Dec;45:2235-44.
46. Maeda N, Li H, Lee D, Oliver P, Quarfordt SH, Osada J. Targeted disruption of the apolipoprotein C-III gene in mice results in hypotriglyceridemia and protection from postprandial hypertriglyceridemia. J Biol Chem. 1994 Sep 23;269:23610-6.
47. Aalto-Setala K, Fisher EA, Chen X, Chajek-Shaul T, Hayek T, Zechner R, Walsh A, Ramakrishnan R, Ginsberg HN, Breslow JL. Mechanism of hypertriglyceridemia in human apolipoprotein (apo) CIII transgenic mice. Diminished very low density lipoprotein fractional catabolic rate associated with increased apo CIII and reduced apo E on the particles. J Clin Invest. 1992 Nov;90:1889-900.
48. Ginsberg HN, Le NA, Goldberg IJ, Gibson JC, Rubinstein A, Wang-Iverson P, Norum R, Brown WV. Apolipoprotein B metabolism in subjects with deficiency of apolipoproteins CIII and AI. Evidence that apolipoprotein CIII inhibits catabolism of triglyceride-rich lipoproteins by lipoprotein lipase in vivo. J Clin Invest. 1986 Nov;78:1287-95.
49. Breyer ED, Le NA, Li X, Martinson D, Brown WV. Apolipoprotein C-III displacement of apolipoprotein E from VLDL: effect of particle size. J Lipid Res. 1999 Oct;40:1875-82.
50. Frenkel B, Bishara-Shieban J, Bar-Tana J. The effect of beta,beta'-tetramethylhexadecanedioic acid (MEDICA 16) on plasma very-low-density lipoprotein metabolism in rats: role of apolipoprotein C-III. Biochem J. 1994 Mar 1;298 (Pt 2):409-14.
51. Blom DJ, O'Neill FH, Marais AD. Screening for dysbetalipoproteinemia by plasma cholesterol and apolipoprotein B concentrations. Clin Chem. 2005 May;51:904-7.
52. Iizuka S, Suzuki W, Tabuchi M, Nagata M, Imamura S, Kobayashi Y, Kanitani M, Yanagisawa T, Kase Y, Takeda S, Aburada M, Takahashi KW. Diabetic complications in a new animal model (TSOD mouse) of spontaneous NIDDM with obesity. Exp Anim. 2005 Jan;54:71-83.
53. Haffner SM, Goldberg RB. New strategies for the treatment of diabetic dyslipidemia. Diabetes Care. 2002 Jul;25:1237-9.
54. Dixon JL, Stoops JD, Parker JL, Laughlin MH, Weisman GA, Sturek M. Dyslipidemia and vascular dysfunction in diabetic pigs fed an atherogenic diet. Arterioscler Thromb Vasc Biol. 1999 Dec;19:2981-92.
55. Jong MC, Dahlmans VE, van Gorp PJ, van Dijk KW, Breuer ML, Hofker MH, Havekes LM. In the absence of the low density lipoprotein receptor, human apolipoprotein C1 overexpression in transgenic mice inhibits the hepatic uptake of very low density lipoproteins via a receptor-associated protein-sensitive pathway. J Clin Invest. 1996 Nov 15;98:2259-67.
56. Wiegman CH, Bandsma RH, Ouwens M, van der Sluijs FH, Havinga R, Boer T, Reijngoud DJ, Romijn JA, Kuipers F. Hepatic VLDL production in ob/ob mice is not stimulated by massive de novo lipogenesis but is less sensitive to the suppressive effects of insulin. Diabetes. 2003 May;52:1081-9.
57. Beckman. Instructions for using the Beckman tube slicer. 1988.
58. Zisman A, Peroni OD, Abel ED, Michael MD, Mauvais-Jarvis F, Lowell BB, Wojtaszewski JF, Hirshman MF, Virkamaki A, Goodyear LJ, Kahn CR, Kahn BB. Targeted disruption of the glucose transporter 4 selectively in muscle causes insulin resistance and glucose intolerance. Nat Med. 2000 Aug;6:924-8.
59. Vergnes L, Baroukh N, Ostos MA, Castro G, Duverger N, Nanjee MN, Najib J, Fruchart JC, Miller NE, Zakin MM, Ochoa A. Expression of human apolipoprotein A-I/C-III/A-IV gene cluster in mice induces hyperlipidemia but reduces atherogenesis. Arterioscler Thromb Vasc Biol. 2000 Oct;20:2267-74.
60. Ebara T, Ramakrishnan R, Steiner G, Shachter NS. Chylomicronemia due to apolipoprotein CIII overexpression in apolipoprotein E-null mice. Apolipoprotein CIII-induced

hypertriglyceridemia is not mediated by effects on apolipoprotein E. J Clin Invest. 1997 Jun 1;99:2672-81.
61. Yoshino G, Tsutomu Hirano, Tsutomo Kazumi. Dyslipidemia in diabetes mellitus. Diabetes Research and Clinical Practice. 1996 March 1996;33:1-14.
62. Bar-On H, Chen YD, Reaven GM. Evidence for a new cause of defective plasma removal of very low density lipoproteins in insulin-deficient rats. Diabetes. 1981 Jun;30:496-9.
63. Bar-on H, Levy E, Oschry Y, Ziv E, Shafrir E. Removal defect of very-low-density lipoproteins from diabetic rats. Biochim Biophys Acta. 1984 Mar 27;793:115-8.
64. Mann CJ, Troussard AA, Yen FT, Hannouche N, Najib J, Fruchart JC, Lotteau V, Andre P, Bihain BE. Inhibitory effects of specific apolipoprotein C-III isoforms on the binding of triglyceride-rich lipoproteins to the lipolysis-stimulated receptor. J Biol Chem. 1997 Dec 12;272:31348-54.
65. Marcoux C, Tremblay M, Fredenrich A, Davignon J, Cohn JS. Lipoprotein distribution of apolipoprotein C-III and its relationship to the presence in plasma of triglyceride-rich remnant lipoproteins. Metabolism. 2001 Jan;50:112-9.
66. Batal R, Tremblay M, Barrett PH, Jacques H, Fredenrich A, Mamer O, Davignon J, Cohn JS. Plasma kinetics of apoC-III and apoE in normolipidemic and hypertriglyceridemic subjects. J Lipid Res. 2000 May;41:706-18.
67. Aalto-Setala K, Weinstock PH, Bisgaier CL, Wu L, Smith JD, Breslow JL. Further characterization of the metabolic properties of triglyceride-rich lipoproteins from human and mouse apoC-III transgenic mice. J Lipid Res. 1996 Aug;37:1802-11.
68. Takahashi T, Hirano T, Okada K, Adachi M. Apolipoprotein CIII deficiency prevents the development of hypertriglyceridemia in streptozotocin-induced diabetic mice. Metabolism. 2003 Oct;52:1354-9.
69. Weinstock PH, Bisgaier CL, Aalto-Setala K, Radner H, Ramakrishnan R, Levak-Frank S, Essenburg AD, Zechner R, Breslow JL. Severe hypertriglyceridemia, reduced high density lipoprotein, and neonatal death in lipoprotein lipase knockout mice. Mild hypertriglyceridemia with impaired very low density lipoprotein clearance in heterozygotes. J Clin Invest. 1995 Dec;96:2555-68.
70. McConathy WJ, Gesquiere JC, Bass H, Tartar A, Fruchart JC, Wang CS. Inhibition of lipoprotein lipase activity by synthetic peptides of apolipoprotein C-III. J Lipid Res. 1992 Jul;33:995-1003.
71. Fung MA, Frohlich JJ. Common problems in the management of hypertriglyceridemia. Cmaj. 2002 Nov 26;167:1261-6.
72. Shachter NS, Ebara T, Ramakrishnan R, Steiner G, Breslow JL, Ginsberg HN, Smith JD. Combined hyperlipidemia in transgenic mice overexpressing human apolipoprotein Cl. J Clin Invest. 1996 Aug 1;98:846-55.
73. Ranganathan G, Li C, Kern PA. The translational regulation of lipoprotein lipase in diabetic rats involves the 3'-untranslated region of the lipoprotein lipase mRNA. J Biol Chem. 2000 Dec 29;275:40986-91.
74. Veerkamp MJ, de Graaf J, Stalenhoef AF. Role of insulin resistance in familial combined hyperlipidemia. Arterioscler Thromb Vasc Biol. 2005 May;25:1026-31.
75. Roden M, Price TB, Perseghin G, Petersen KF, Rothman DL, Cline GW, Shulman GI. Mechanism of free fatty acid-induced insulin resistance in humans. J Clin Invest. 1996 Jun 15;97:2859-65.
76. Mingrone G, Henriksen FL, Greco AV, Krogh LN, Capristo E, Gastaldelli A, Castagneto M, Ferrannini E, Gasbarrini G, Beck-Nielsen H. Triglyceride-induced diabetes associated with familial lipoprotein lipase deficiency. Diabetes. 1999 Jun;48:1258-63.
77. Harmon JS, Gleason CE, Tanaka Y, Poitout V, Robertson RP. Antecedent hyperglycemia, not hyperlipidemia, is associated with increased islet triacylglycerol content and decreased insulin gene mRNA level in Zucker diabetic fatty rats. Diabetes. 2001 Nov;50:2481-6.
78. Matsui H, Okumura K, Kawakami K, Hibino M, Toki Y, Ito T. Improved insulin sensitivity by bezafibrate in rats: relationship to fatty acid composition of skeletal-muscle triglycerides. Diabetes. 1997 Mar;46:348-53.

79. Andersson Y, Majd Z, Lefebvre AM, Martin G, Sechkin AV, Kosykh V, Fruchart JC, Najib J, Staels B. Developmental and pharmacological regulation of apolipoprotein C-II gene expression. Comparison with apo C-I and apo C-III gene regulation. Arterioscler Thromb Vasc Biol. 1999 Jan;19:115-21.
80. Mitchell BD, Kammerer CM, Blangero J, Mahaney MC, Rainwater DL, Dyke B, Hixson JE, Henkel RD, Sharp RM, Comuzzie A, Vandeberg J, Stern M, MacCluer, J. Genetic and environmental contributions to cardiovascular risk factors in Mexican Americans. The San Antonio Family Heart Study. Circulation. 1996 Nov 1;94:2159-70.

APPENDIX

Hepatic VLDL-TG production in vivo.

1. Fast mice overnight.
2. Weigh mice before injection.
3. Inject intraperitoneally with 500 mg of Triton WR 1339; plasma VLDL clearance is completely inhibited under these conditions.

Preparation of Triton WR 1339:

1. Weigh out 100 mg of tyloxopol (about 3 drops).
2. Load 0.9% NaCl (saline) up to 1 ml/1000 µl mark of 1.5 ml microcentrifuge.
3. Mix by pipetting up and down.

4. Collect blood via the retro-oribtal plexus at 0, 1, 2, 3, and 4 hour time points after the injection.
5. Centrifuge for 10 minutes at 4000 x g at 4ºC
6. Determine plasma triglyceride levels by assay.

[Next, 5 µl VLDL and 2 ml solvable were loaded into a disposable scintillation vial. 10 ml of scintillation fluid (Eco Lite) was then loaded into the vial and gently mixed. One hour later, the VLDL levels were measured using the Beta Counter in disintegrations per minute (DPM).] PUT [ ] IN YOUR APPENDIX.

Hepatic VLDL-TG clearance in vivo.

Day 1:

1. Inject 100 µl of [^{3}H] palmitic acid into tail vein.

Preparation of [^{3}H] palmitic acid:

1. Make 200 µl/200 ml for 20 mice.
2. Working solution is 1mCi so 1 mCi/.85 (stock) = 1.17 ml
3. For 20 mice, .117 ml x 20 = 2.34 ml
4. Load 2.34 ml of [^{3}H] palmitic acid into 15 ml tube.
5. Evaporate ethanol by nitrogen gas (about 1.5 hours).
6. Redissolved by loading 2 ml of 0.9% NaCl and 4 mg/ml of BSA powder into 15 ml tube.

2. Do cardiac puncture (bled from the abdominal aorta) 25 minutes after injection.
3. Centrifuge for 11 minutes at 1200 x g at 4ºC (until you see plasma).
4. Load 2.4 µl of plasma and 9.6 ml NaCl and KBr solution to a 12 ml polyallomer centrifuge tubes.

   Preparation of NaCl and KBr solution:

   1. Weigh out 15.3 g NaCl and dissolve into 100 ml sterilized deoionized water.
   2. Weigh out 35.4 g KBr and dissolve into 100 ml sterilized deoionized water.
   3. Need a final concentration of .65% and 1.52%.
      a. 15.3 x X = 0.65 x 100 = 65/15.3 = 4.25 ml NaCl
      b. 35.4 x X = 1.52 x 100 = 152/35.4 = 4.29 ml KBr
      c. Measure NaCl and KBr respectively and 0.9% NaCl is added to make the final concentration of 100 ml in a volumetric flask.
      d. A density < 1.019 is needed.
   1. Weight of the volumetric flask before: 61.49g
   2. Weight of the volumetric flask after: 163.01 g
   3. 163.01 – 61.49 = 101.52/100 = 1.0152 (density < 1.019)

5. Ultracentrifuge plasma with NaCl and KBr solution for 16 hours at 40,000 x g at 4ºC.

Day 2:

1. Slice the tube (using the tube slicer) and withdrawal liquid (VLDL) from the top portion (~1.5cm) of tube using a syringe or pipette. Remove the sliced off portion of the tube and pull the blade out.
   See directions using the Tube Slicer.
2. Measure 5 µl and 2 ml of solvable and load contents into a disposable scintillation vial.
3. Load 10 ml of scintillation fluid (Eco Lite) into a vial, mix and wait about 1 hour.
4. Count using the Beta-Counter in disintegrations per minute (DPM).
5. Inject 100 µl of radiolabeled VLDL into each fasted mouse (overnight).
   Preparation of radiolabeled VLDL:
   1. Measure 1848 µl of 0.9% NaCl (saline) and 552 µl of VLDL.
6. Collect blood via the retro-oribtal plexus at 5, 10, 15, 20 minute time points after the injection.
7. Centrifuge for 10 minutes at 4000 x g at 4ºC.
8. Measure 10 µl of plasma and 4 ml of solvable and load into vial.
9. Load 10 ml of scintillation fluid into vial and allow to mix with the plasma.
10. Dissolve for a few minutes.
11. Count VLDL using Beta-Counter.

Northern blot analysis

Total RNA Extraction from liver tissue using the RNeasy Midi Kit (Qiagen, Valencia, CA).

1. Homogenize frozen liver tissue in 10 ml tube with 6 ml of Buffer RLT and 60 µl of Beta-Mercaptoethanol (B-ME). Use under fume hood.
2. Cap the tube securely and shake it by hand vigorously for 15 seconds.
3. Centrifuge for 10 minutes at 3400 x g at 22ºC.
4. Transfer the lysate to a new 15 ml test tube by pipetting.
5. Load 6 ml of 70% ethanol in DEPC treated water to the lysate and mix immediately by shaking vigorously to avoid RNA contamination.
6. Without delay, apply the sample to an RNeasy midi column placed in the 15 ml centrifuge tube (supplied).
7. Close the tube gently.
8. Centrifuge for 5 minutes at 3400 x g at 22ºC.
9. Discard the flow-through.
10. Repeat steps 6-9, using the remainder of the sample (up to 4 ml).
11. Load 4 ml of Buffer RW1 to the RNeasy column.
12. Close the tube gently.
13. Centrifuge for 5 minutes at 3400 x g at 22ºC to wash the column.
14. Discard the flow-through.
15. Load 2.5 ml of Buffer RPE to the RNeasy column.
16. Close the tube gently.
17. Centrifuge for 2 minutes at 3400 x g at 22ºC.
18. Discard the flow-through.
19. Load another 2.5 ml of Buffer RPE to the RNeasy column.
20. Close the tube gently.
21. Centrifuge for 5 minutes at 3400 x g at 22ºC to dry the RNeasy silica-gel membrane
22. Discard the flow-through.

Note: it is important to ensure that the RNeasy membrane is dry since residual ethanol may interfere with downstream reactions.

23. To elute, transfer the RNeasy column from the centrifuge tube very carefully to a new collection tube (supplied).
24. Load 250 µl of RNase-free water directly onto the RNeasy silica-gel membrane.
25. Close the tube gently.

26. Let it stand for 1 minute.
27. Centrifuge for 3 minutes at 3400 x g at 22ºC.
28. Do not discard.
29. Repeat the elution step with a second volume (250 µl) of RNase-free water. This wash the release more RNA.
30. Load the RNA volume (500 µl) to a new microcentrifuge.
31. Load 50 µl of Sodium Acetate 3M in DEPC treated water into the microcentrifuge.
32. Vortex using the Type 16700 Mixer.
33. Load 500 µl of isopropanol into the microcentrifuge.
34. Invert microcentrifuge.
35. Centrifuge for 20 minutes at 13000 x g at 4ºC.
36. Carefully discard the solution and load 500 µl of 70 % ethanol in DEPC treated water into the microcentrifuge.
37. Allow pellet to dry completely under fume hood for 5 minutes.
38. Load 15 µl of RNase free water to the sample and vortex until is pellet is dissolved.
39. Quick spin and vortex.
40. Load 10 µl of formamide, 3.6 µl of formaldehyde, 2 µl of 10X Mops, 2.4 µl of RNase free water, and 2 µl of RNA into a new microcentrifuge.
41. Store preparation into incubator for about 15 minutes.
42. Store RNA at –80 ºC.
43. After incubation, transfer microcentrifuge into ice chest for about 15 minutes.
44. Centrifuge for a few seconds.

Gel Electrophoresis

Preparation of 1 % agarose/2.2M agarose gel:

1. Weigh .5 g agarose.
2. Mix agarose with 36 ml sterilized deionized water in a baked (autoclave) flask.
3. Microwave until agarose is cooked (about 25 seconds).
4. Remove flask from microwave and shake.
5. Return flask to microwave and heat again (about 10 seconds).
6. Cool gel solution in fume hood.
7. Add 5 ml of 10X MOPS to gel solution.
8. Add 9 ml of formaldehyde to gel solution and shake. Formaldehyde is added to denature the RNA and make it run true to size.
9. Set up cast, making sure to add the comb (creates wells for the RNA).
10. Pour gel solution into cast.
11. Set until gelled (about 1 hour).
12. Carefully pour buffer solution into the over the electrophoretic gel box trying to minimize bubbles.
13. Remove comb.

Preparation of samples to load on gel.

1. Samples will have a final volume of 20 µl.
2. Add 3 µl dye into each sample and load into wells.
3. Run gel from negative to positive at 100 volts for 1 hour (times may vary).
4. After running the gel, carefully transfer the gel into a plastic staining container.
5. Pour deionized water (around 100 ml) over the gel.
6. Load 5 µl of ethidium bromide into the plastic staining container.
7. Stain for 10 minutes using lab rotator.
8. Pour ethidium bromide waste into glass jar.
9. Destain gel from 30 minutes to overnight by pouring deionized water over gel into the plastic container (about 2/3).
10. Capture the image of the gel using the High Performance Ultra Illuminator.

Directions using the High Performance Ultra Illuminator

1. Carefully transfer the gel from container to High Performance Ultra Illuminator.
2. Close door.
3. Select Kodak 1DLE 3.5.
4. Select Capture.
5. Select SYBR Green.
6. Select 20.5 x 28 cm.
7. Select 3.5 sec.
8. Select on.
9. Take picture.
10. When processing image, select off.
11. Close.
12. Save as Jpeg file.
13. Image display.

Preparation of buffer for gel solution

1. Load 25 ml of 10X MOPS to a baked cylinder.
2. Mix with 225 ml of sterilized deionized water.
3. Parafilm is used as a lid for the cylinder.
4. Invert buffer solution.

Transfer to a Hybond N+ (membrane) (Amersham Piscataway, NJ).

1. Take white plastic staining dish and fill with buffer solution containing 20 X SSC (about 500 ml).
2. Use yellow gel plate (medium sized gels) and turn upside down and place over staining dish perpendicularly.
3. Make 2 long strips of Watmann paper. They should be long enough to drape over the gel plate and into the 20 X SSC on both sides. They should be wide enough to fit the size of the gel to be transferred and have some extra space on the top and bottom.
4. Set a glass over the gel plate containing the buffer solution.
5. Position the 2 long strips of Watmann paper over the glass—folding down the sides and making sure that wick is saturated in the buffer solution.
6. Position the gel to be transferred flipped on the top of the papers and smooth out all air bubbles.
7. Using saran wrap, cover all 4 sides of the papers, gel plate, and staining dish. The only thing that should be left uncovered is the gel.
8. Place the membrane on top of the gel and smooth out all air bubbles.
9. Wet 2 pieces of the cut Whatmann paper with sterilized deoinozied water and place on top of the membrane (remove all air bubbles).
10. Place 3 dry gel sized Whatmann papers on top of the wet ones.
11. Stack 4.5 inches of folded white paper towels (cut in half) on top of the Whatmann papers.
12. Place another glass over the white paper towels.
13. Add a weight to the top of the glass. Usually a Sigma catalog book is sufficient. Make sure weight is balanced, so it does not fall over throughout the night.
14. Set overnight.

Hybridize overnight with random primed α-^{32}P-labeled Apo C-III cDNA probe.

1. Next day uncover everything down to the membrane. Be careful only to touch outside edges of the membrane.
2. Poke holes in the membrane corresponding to each well on the gel. Then carefully flip membrane over and cut the upper hand left corner.

3. Carefully place the membrane in a white weighing boat and use UV machine to expose the membrane for 2 minutes.
4. Use a pencil and write what is in each lane on top of the membrane.
5. Then wrap completely in saran wrap and store until ready to label.

Directions on using the DNA transfer lamp:

1. Select on.
2. Open door.
3. Slide in weighing boat containing the membrane.
4. Set start: 2 minutes.

Pre-hybridization

1. Set hybridization oven at 65ºC.
2. Place rapid hybridization buffer in the oven—warming until temperature reaches 65ºC (about 20 minutes).
3. Place mesh (same size as membrane) and the membrane in a small boat containing 100 ml of 2 X SSC.
4. Add 7 ml of rapid hybridization buffer to a glass bottle.
5. Roll membrane on top of mesh and carefully set in the glass bottle containing the rapid hybridization buffer. Use large forceps and do not touch the inside of the membrane.
6. Slowly unroll the membrane in the glass bottle, and eliminate air bubbles.
7. Set bottle in hybridization oven from 2 hours to overnight.

Rediprime II Random Prime Labeling System (Amersham).

1. Mix 15 µl of APO C III probe and 33 µl of TE buffer into a new microcentrifuge.
2. Denature the DNA sample by heating to 100 ºC for 5 minutes in heating block.
3. Immediately place the DNA sample in ice chest for 5 minutes.
4. Vortex and quick spin the contents.
5. Add the denatured DNA (45 µl) to the rediprime (reaction tube).
6. Add 5 µl of 32-phosphorous (32-P) to the rediprime.
7. Gently agitate by flicking tube until solution is dissolved.
8. Quick spin.
9. Incubate at 37 ºC for 10 minutes.
10. Stop the reaction by loading 5 µl of 0.2 M EDTA into the rediprime.
11. Denature the labeled DNA by heating at 100 ºC for 5 minutes and then snap cool on ice for 5 minutes.
12. Load 60 µl of DNA sample into the bottle.
13. Place the bottle back in hybridization over overnight.

Wash blots

1. Take bottle out of hybridization oven.
2. Pour solution in waste (32-P) bucket. Do everything in fume hood.
3. Use forceps to remove the mesh and membrane out of bottle and transfer into large plastic container containing 2 X SSC/0.5% SDS (about 350 ml). This is the first wash.

Preparation of 2 X SSC/0.5% SDS: 100 ml of 20 X SSC + 5 ml SDS.

4. Place plastic container in water bath (set at 65 ºC) for 20 minutes.
5. Make sure to place weights over the container.
6. Pour washing solution in sink, keeping both the mesh and membrane in container.
7. Add .5 X SSC/0.5% SDS solution in the container. This is the second wash.

Preparation of .5 X SSC/0.5% SDS: 25 ml of 20 X SSC + 5 ml SDS).

8. Place plastic container in water bath (set at 65 ºC) for 20 minutes.
9. Make sure to place weights over the container.
10. Pour washing solution in sink, keeping both the mesh and membrane in container.
11. Add .1 X SSC/0.5% SDS solution in the container. This is the third wash.

Preparation of .5 X SSC/0.5% SDS: 5 ml of 20 X SSC + 5 ml SDS).

12. Place plastic container in water bath (set at 65 ºC) for 20 minutes.

13. Make sure to place weights over the container.
14. Pour washing solution in sink, keeping both the mesh and membrane in container.
15. Remove membrane from container and lay over wick type paper for drying, but do not let membrane deep dry.
16. Carefully wrap membrane in saran wrap.
17. Place the membrane in audioradiography cassette (intensifying screen) and secure membrane by taping the bottom and top sides of the saran wrap.
18. Place mesh in white paper towels.
19. Take out the film box and bring to dark room along with the membrane enclosed in the audioradiography and intensifying screen.
20. In dark room, place film in the screen and close.
21. Store the audioradiography and intensifying screen in –80 ºC for 30 minutes to overnight (exposure times vary).
22. Take screen out of –80 ºC storage and bring to dark room.
23. Open screen and place film through the developer.
24. When finished take film out.

Instructions for operating the developer:
Warming up:
1. Close the wash water drainage valve, making sure that the developer and fixed drainage valves are closed.
2. Turn on the power beaker on the right side of developer. You will see the RUN button lamp goes on.
3. Press the Run button. The Run lamp will light up to indicate the SRX-101A is operation. It will automatically go out if no film has been inserted for 8 hours.
4. Close the feed tray cover.
5. Wait for 20-30 minutes until the ready lamp lights up. The SRX-101A is ready for film processing.

Inserting film:
1. Make sure that the Ready lamp is ON.
2. Open the feed tray cover.
3. Insert film, always lining up the film edge to either right or left guide located on the feed tray.
4. After the leading edge of the film is grabbed by the roller, the film will be automatically fed into the developer.
5. The ready lamp will go out.
6. When a ready signal (beep) sounds and the ready lamp goes on again (10 sec) you can insert next film.

Shutting down:
1. Press the RUN button. The run lamp will go out.
2. Open the water drainage valve. Leave the developer and fixer drainage valves closed.
3. Open the feed tray cover to prevent condensation inside the main unit.
4. Turn off the power breaker.

Preparation of 20 X SSC in DEPC treated water

15. Mix 175 g of sodium chloride (NaCl) and 8 g of sodium citrate (Na_3 citrate) in 1000 ml of DEPC treated water.

Total RNA Extraction by RNeasy Midi Kit (Qiagen, Valencia, CA) for real time RT PCR.

1. Homogenize frozen adipose tissue in 50 ml tube with 15 ml QIAzol Lysis Reagent.

2. Place the tube containing the homogenate on the benchtop at room temperature (25ºC) for 5 minutes.
3. Add 15 ml Chloroform, cap the tube securely and shake it by hand vigorously for 15 seconds to extract excess lipids.
4. Place the tube containing the homogenate on the benchtop at room temperature (25ºC) for 2-3 minutes.
5. Centrifuge at 3400 x g for 20 minutes at 4ºC.
6. Transfer upper aqueous phase to a new 15 ml tube.
7. Add an equal volume of step 6 of 70% ethanol, and mix thoroughly by vortexing. Do not centrifuge. Continue without delay.
8. Pipet up to 4 ml of the sample into an RNeasy Midi Spin Column in a 15 ml collection tube (supplied). Close the tube gently.
9. Centrifuge for 5 minutes at 3400 x g at 25ºC.
10. Discard the flow-through.
11. Repeat steps 8-10, using the remainder of the sample (up to 4 ml).
12. Add 4 ml Buffer RW1 to the RNeasy Midi Spin Column. Close the tube gently.
13. Centrifuge for 5 minutes at 3400 x g at 25ºC to wash the column.
14. Discard the flow-through.
15. Add 2.5 ml Buffer RPE to the RNeasy Spin Column. Close the tube gently.
16. Centrifuge for 2 minutes at 3400 x g at 25ºC to wash the column.
17. Discard the flow-through.

Note: Buffer RPE is supplied as a concentrate. Make sure that 95% ethanol is added to Buffer RPE before use.

18. Add another 2.5 ml Buffer RPE to the RNeasy Spin Column. Close the tube gently.
19. Centrifuge for 5 minutes at 3400 x g at 25ºC to dry the RNeasy silica-gel membrane.

Note: It is important to dry the RNeasy silica-gel membrane since residual ethanol may interfere with downstream reactions. This step ensures that no ethanol is carried over during elution.

20. Carefully remove the RNeasy Midi Spin from the collection tube so the column does not contact the flow through as this will result in carryover of ethanol.
21. To elute, transfer the RNeasy Midi Spin Column to a new 15 ml collection (supplied).
22. Pipet 100 µl of RNase free water directly onto the RNeasy silica-gel membrane. Close the tube gently.
23. Let the tube stand for 1 minute.
24. Centrifuge for 3 minutes at 3400 x g at 22ºC
25. Repeat steps 22-24. Elute into the same collection tube. This wash will release more RNA.
26. After centrifugation, pipet the 200 µl to a new microcentrifuge.
27. Add 20 µl of Sodium Acetate 3M in DEPC treated water into the solution.
28. Vortex the microcentrifuge using the Type 16700 Mixer.
29. Add 200 µl of isopropanol into the microcentrifuge.
30. Invert the microcentrifuge.
31. Centrifuge at 13,000 x g at 4ºC for 20 minutes.
32. After centrifugation, a pellet should form. Carefully discard the supernatant solution onto kim wipes.
33. Re-suspend pellet in 200 µl of 70% ethanol in DEPC treated water into the microcentrifuge.
34. Carefully close the lid and vortex.
35. Centrifuge at 13,000 x g at 4ºC for 10 minutes.
36. Discard the solution and allow pellet to dry completely under fume hood for 5 minutes.
37. Re-suspend pellet in 10 µl of RNase-free water into the microcentrifuge.
38. Vortex until pellet is dissolved.

Quantification of RNA by Nano-drop (ND)

1. On the computer, select ND-1000 program.

2. Select nucleic acid.
3. Load 1 µl of DEPC treated water onto ND to initiate.
4. Select OK.
5. Change the program to RNA-40.
6. Pull the handle down.
7. Clean the ND with kim wipe.
8. Select blank.
9. Pull the handle down.
10. Type in sample ID.
11. Flick tube with sample.
12. Load 1 µl of RNA to ND.
13. Pull handle down.
14. Select measure.
15. Print report and exit.

RNA →→ cDNA

1. Load 2 µg RNA and RNase free water to add up to 12 µg concentration to 1.5 ml tube.
2. Load 2 µl oligo dT primer into tube with RNA and RNase free water.
3. Load 2 µg RNA of each sample to reference tube with RNase free water.
4. Gently tap tube to vortex.
5. Turn on PCR machine.
6. Select program.
7. Select list: cDNA.
8. Close lids of PCR machine.
9. Run PCR machine at 70 ºC for 10 minutes.
10. Pause at 70 ºC.
11. Immediately set samples on ice for 1 minute.
12. Prepare reagents while samples are in PCR machine.
13. Spin down reagents.
14. Load 1 µl of dNTPs, 2 µl of 0.1 M DTT, 4 µl of 5 X buffer synthesis, and 1 µl of SSII RT (superscript enzyme) into new 1.5 ml tube.
15. Gently tap tube to vortex.
16. Add reagents to RNA tube.
17. Gently tap tube to vortex.
18. Close lids of PCR machine.
19. Resume PCR machine (select pause) at 25 ºC for 10 minutes, 42ºC for 50 minutes, and 70ºC for 15 minutes.
20. Immediately set samples on ice for 1 minute.
21. Load 20 µl of prepared samples into new 1.5 ml tube.
22. Store cDNA at -20 ºC for short term.

cDNA for RT real time PCR:

Dilutions:
1. Add 20 µl of RNAase free water to each tube (5 total).
2. Add 5 µl of cDNA to tube #1.
3. Transfer 1 µl solution from tube #1 to tube #2. Flick.
4. Transfer 1 µl solution from tube #2 to tube #3. Flick
5. Transfer 1 µl solution from tube #3 to tube #4. Flick
6. Transfer 1 µl solution from tube #4 to tube #5. Flick

1. Add 1 µl of diluted cDNA into each sample tube.

2. Add 10.5 µl of RNAase free water into each tube.
3. Add 1 µl of RT^2 PCR Primer Set (LPL, 18S-Super Array) into each tube.
4. Add 12.5 µl of RT PCR Master Mix into each tube.
5. Add 25 µl solution from each tube into each well of the Thermo-Fast 96 Detection Plate (catalog # AB-1307)
6. Using the Adhesive Seal Applicator (part # 436 5988 AB) drape optical adhesive cover (part # 431197 AB) over well plate.
7. Place well plate into computer to begin RT Real Time PCR.

Set-up
Well Inspector

Use	Detector	Reporter	Quencher	Task	Quantity	Color
Check	LPL/18S	SYBR	None	Unknown	Blank	Black

Passive Reference: ROX
To Generate Standard Curve

Use	Detector	Reporter	Quencher	Task	Quantity	Color
Check	LPL/18S	SYBR	None	Standard	625	Black
Use	Detector	Reporter	Quencher	Task	Quantity	Color
Check	LPL/18S	SYBR	None	Standard	125	Black
Use	Detector	Reporter	Quencher	Task	Quantity	Color
Check	LPL/18S	SYBR	None	Standard	25	Black
Use	Detector	Reporter	Quencher	Task	Quantity	Color
Check	LPL/18S	SYBR	None	Standard	5	Black
Use	Detector	Reporter	Quencher	Task	Quantity	Color
Check	LPL/18S	SYBR	None	Standard	1	Black

Instrument:
Thermal Profile
‘

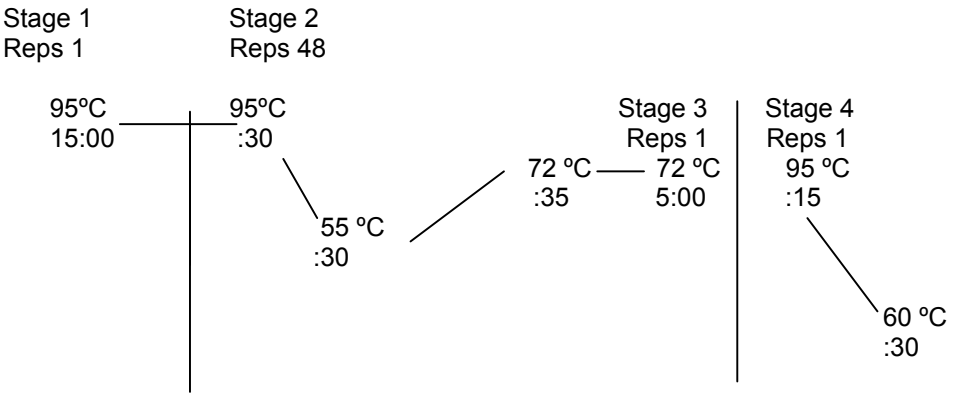

SPECTROMETER

1. Turn machine on.
2. Press 1.
3. Set up test and select 3 for wavelength. Read glucose at 500 nm and triglyceride at 540 nm.
4. Select enter and 3 again.
5. Place deoionized water reference in #1 well. Make sure the arrow on the cuvet is pointing left. (7 cuvettes total; order: water, then standard, then duplicate.
6. Select cell down, B-blank
7. Auto zero (to change wavelengths).
8. Cell up-well #2.
9. Select measure.
10. Select measure again.
11. Discard cuvettes after reading absorbencies

GLUCOSE ASSAY

1. Prepare the glucose reagent if necessary; load 50 ml of sterile deoionized water into cylinder to make up solution.
2. Set up enough cuvettes for standards and samples, include duplicates of each.
3. Load 900 μl of glucose reagent to each cuvet, including standards (0 mg/dl: water blank, 25 mg/dl, 50 mg/dl, 75 mg/dl, and 100 mg/dl) and samples.
   A. For the standard cuvettes, do not dilute; using M10 pipette, load 6 μl of standard to cuvettes; wash tip of pipette after each time, including duplicates; quick spin and vortex the standards before use.
   B. For the sample cuvettes (and duplicates): dilute; using M10 pipette, load 4 μl of sterilized deoionized water to cuvet; next load 2 μl of plasma to each cuvet; do not forget to wash tip of pipette.
4. Vortex all cuvettes.
5. Allow cuvettes to incubate for 10-15 minutes at room temperature.
6. Use Spectrometer-should be set at 500 nm.

TRIGLYCERIDE ASSAY

1. Prepare the Free Glycerol Reagent and the Triglyceride (TG) Reagent according to the preparation instructions
   A. Free Glycerol is 40 ml; TG reagent is 10 ml.
2. Warm up the spectrometer and set it to read OD of 540 nm and auto zero with water.
3. Warm up the Free Glycerol Reagent to room temp before starting the assay (all reagents need to be kept in -20 ºC when not in use).
4. Set up enough cuvettes for a blank, standards, and all samples. No duplicates for samples
5. Load 640 μl of the Free Glycerol Reagent into each cuvet-set epindorf to 2 (this is 500 μL); for the rest of the 640 μl, load 140 μl into the cuvettes using the blue tips.
6. Load 8 μl of water to the blank, 8 μl of the 250 mg glycerol standard to one cuvet and 8 μl of the 500 mg glycerol standard to the other standard cuvet; load 8 μl of plasma (from samples) to cuvettes; use M10 (red pipette).
7. Vortex samples, and allow to incubate for 10-15 minutes at room temperature.
8. Read and record the initial absorbance (IA) of the blank, standards, and samples versus water as the reference (just add deionized water to a random cuvet).
9. Load 160 μl of the TG reagent into each cuvet, vortex, and incubate at room temperature for 10-15 minutes.

10. Read and record absorbance (FA) of blank, standards, and samples versus water as the reference.
11. Calculate the concentrations of glycerol, true TG, and total TG in the sample.

CHOLESTEROL ASSAY

1. Add 200 μl of sterile deoinized water to first well.
2. Add 200 μl of reagent (standard-Infinity Cholesterol) to second well.
3. Add 200 μl of reagent (std) + 2μl of sterile deoinized water to third well.
4. Add 200 μL of reagent (std) + 2 μl of sample to fourth well.
5. Then load all samples to wells- 2 μl.
6. No duplicates.
7. Allow to incubate at room temperature—drape a kim wipe over it.
8. Mix the wells.

INSULIN ASSAY

Day 1:

1. White towel on lab bench
2. Close window when opening buffer-powder
3. Add buffer into I-125
4. Make waste bags (2)—throw away buffer into waste bag
5. Fold down over 2nd bag
6. Leave I-125 in hood

Keep samples on ice

7. Label tubes—samples beginning with tube #25

4 samples (#25, 27, 29, 31) duplicates or no duplicates

1. Label tubes (standards 1-24) (no duplicates)
2. Add to sample tubes first: 25 μL buffer into sample tubes (using repeating pipette), then add 25 μL of each sample to tube, using L100 pipette. Start with tube #25. Place sample into tube; flick tube by hand—mixing tube, do not vortex, then pipette into tube.
3. Step 1 pg 10

a. 1, 2 blank; 3 and 4 add buffer assay, 100 μL; 5 & 6 add buffer assay, 50 μL; leave everything else blank.
b. Steps 2 & 3; do what it says leave 1-6 blank; 7 thru 24-50 μL of reagent

Make sure to hit the wall of tube with pipette.
Everything can be done at bench.

In hood.

1. Step 4: Set epindorf to 1—I 125 Insulin tracer (red solution); add 50 μL to all tubes; 1 push (std + samples) just follow directions (no. 1-4); throw away tube (on epindorf using bag as a glove or use kim wipes)
2. Step 5: add 50 μL of insulin AB starting with tube 5 (blue solution).
3. Step 6: Vortex two tubes at a time. Cover with aluminum foil and put radioactive label on top. And write I-125 using black marker. Incubate at 4 degrees; put labels on fridge too. Incubate 20-24 hrs.

Day 2:

1. Remove samples from fridge (incubation)

2. Using epindorf (set to 2) add precipitating reagent-0.5 mL (green soln) to tubes; don't do anything to tubes 1 and 2.
3. Vortex all tubes (~5 sec)
4. Get centrifuge ready.
    a. If needed, 6 min at 500 RPM for 4 degrees. Press green button.
    b. Make sure yellow racks fit in machine (1 rack can hold 37 tubes)
5. Take yellow racks to hood (prepare here for centrifuging)
6. Landmark numbers on top. Start with tube #3. Leave 1 and 2 out.
7. Carefully place samples in yellow rack.
8. Need a Balance?
    a. 650 µL of tap water for balance
9. Centrifuge samples at 3000 RPM for 21 minutes at 4 degrees. Press start.

While centrifuging:

10. Prepare to decant the supernatant (the soln on top); you want to see the pellet on bottom
    a. White towels
    b. Add kim wipes (~20-30)
11. Remove samples when finished centrifuging. Don't disturb.
12. Place samples (in order) into rack (day 2 rack-rack holds 90 samples); start in 2nd row
13. Flip (invert) rack over slowly
14. Fold over the 1st white towel and lay rack on top of it
15. Use kim wipes to transfer tubes into other rack (rack that was used in day 1). Carefully wipe tube with kim wipe
    --if pellet is on side of tube, something went wrong.
16. Throw away white towel (with solution) into waste bag.
17. Computer (reading)
    a. Use machine on the right (w/ comp)—this is gamma.
18. Place tubes in order (remember samples read backwards) into gray rack.
19. On the 15th tube—slide #2 protocol into this tube; this is the 1st rack
20. Place all racks (in order) into/over dent—underneath computer.
21. Place stop rack after all racks at end.
22. Computer:
    a. F2
    b. F5-count
    c. Make sure Power is ON
    d. Make sure On Line is green
    e. If can't read (someone is using machine, etc) leave samples covered in hood
23. Clean up-wash rack with water in radiation sink
24. After finished with calculations (1.5 hrs to read all samples), discard all samples.

VITA

Jennifer Melanie “Pittsburgh” Fortuna was born in Athens, Tennessee on October 3, 1981. She received her Bachelor of Science in Nutrition from the University of Tennessee-Knoxville. Graduate study in the field of nutrition was also completed at the University of Tennessee. Jennifer is finishing up in Knoxville with her dietetic internship, which will be completed in August. She loves God, her family, her friends, and the Pittsburgh Steelers. She also hopes to move to Pittsburgh someday.

“Don't be anxious about tomorrow. God will take care of your tomorrow too. Live one day at a time."

~ Matthew 6:34

“Don’t worry.” **~ Melanie Fortuna** (my Mother)

“Perseverance, and not intelligence, will win out in the end." **~ June Gorski** (a professor)

“Jenny’s just like Kenny.” She’ll eat anything.” **~ Cindy Carlson** (my Godmother)